



The Chemical Interactions of Actinides in the Environment

Wolfgang Runde

From a chemist's perspective, the environment is a complex, particularly elaborate system. Hundreds of chemically active compounds and minerals reside within the earth's formations, and every patch of rock and soil is composed of its own particular mix. The waters that flow upon and through these formations harbor a variety of organic and inorganic ligands. Where the water meets the rock is a poorly understood interfacial region that exhibits its own chemical processes.

Likewise, from a chemist's point of view, the actinides are complex elements. Interrupting the 6d transition elements in the last row of the periodic table, the actinides result as electrons fill the 5f orbitals. Compared with the 4f electrons in the lanthanide series, the 5f electrons extend farther from the nucleus and are relatively exposed. Consequently, many actinides exhibit multiple oxidation states and form dozens of behaviorally distinct molecular species. To confound matters, the light actinides are likely to undergo reduction/oxidation (redox) reactions and thus may change their oxidation states under even the mildest of conditions. Uranium, neptunium, and especially plutonium often display two or

more oxidation states simultaneously in the same solution. Accordingly, the light actinides exhibit some of the richest and most involved chemistry in the periodic table.

As a result, the chemical interactions of actinides in the environment are inordinately complex. To predict how an actinide might spread through the environment and how fast that transport might occur, we need to characterize all local conditions, including the nature of site-specific minerals, temperature and pressure profiles, and the local waters' pH, redox potential (Eh), and ligand concentrations. We also need a quantitative knowledge of the competing geochemical processes that affect the actinide's behavior, most of which are illustrated in Figure 1. Precipitation and dissolution of actinide-bearing solids limit the upper actinide concentration in solution, while complexation and redox reactions determine the species' distribution and stability. The interaction of a dissolved species with mineral and rock surfaces and/or colloids determines if and how it will migrate through the environment.

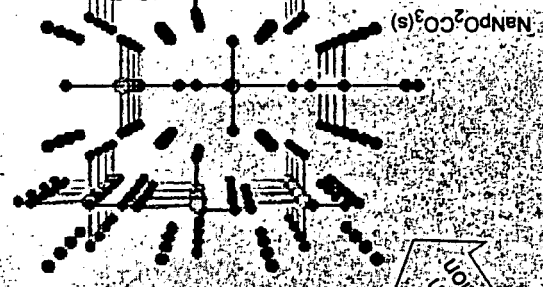
Understanding this dynamic interplay between the actinides and the environment is critical for accurately as-

sessing the feasibility of storing nuclear waste in geologic repositories. The actinides¹ are radioactive, long-lived, and highly toxic. Over the last few decades, vast quantities of transuranic actinides (those with atomic numbers greater than that of uranium) have been produced inside the fuel rods of commercial nuclear reactors. Currently, most spent fuel rods are stored above-ground in interim storage facilities, but the plan in the United States and some European countries is to deposit this nuclear waste in repositories buried hundreds of meters underground. The Department of Energy (DOE) is studying the feasibility of building a repository for high-level waste in Yucca Mountain (Nevada) and has already licensed the Waste Isolation Pilot Plant (WIPP) in New Mexico as a repository for defense-related transuranic waste. Given the actinides' long half-lives, these repositories must isolate nuclear waste for tens of thousands of years.

¹Although "actinides" refers to the fourteen elements with atomic numbers 90 through 103 (thorium through lawrencium), in this article we limit the term to refer only to uranium, neptunium, plutonium, americium, and curium, unless stated otherwise. These five actinides are the only ones that pose significant environmental concerns.

Y 24

2



At low actinide concentrations, sorption onto particulates, clays, or rock surfaces determines the environmental behavior. Actinides can also diffuse into rock, or coprecipitate with natural ligands and become incorporated into minerals.

Np(V) complex sorbed to montmorillonite

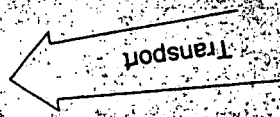
Solvated actinide species can precipitate, forming a solid that in turn determines the upper concentration limit for the solvated species.



Actinides typically form large molecular complexes in solution. Neptunium assumes the Np(V) species, $\text{NpO}_2(\text{H}_2\text{O})_8^{4+}$ in many natural waters.

Microbes can facilitate actinide redox processes, while sorption or uptake by the microbes may be a potential transport or immobilization mode.

Actinides can migrate by water transport or by sorption onto mobile particulates or colloids.



Bioavailability

Redox reactions change an actinide's oxidation state and help to establish equilibrium between species.



The Np(IV) species $\text{Np}(\text{H}_2\text{O})_8^{4+}$

Complexation with different ligands can stabilize actinides in solution and enhance their transport through the environment.

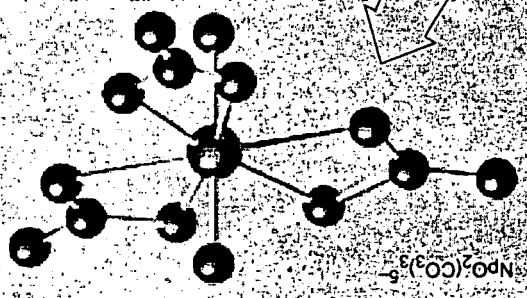


Figure 1: Overview of Actinide Behavior in the Environment

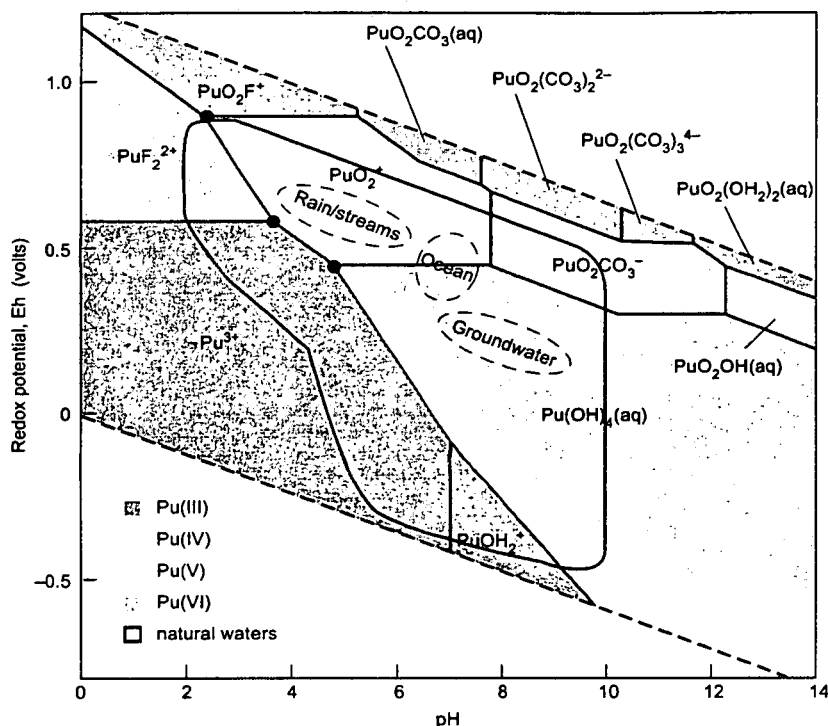


Figure 2. Pourbaix Diagram for Plutonium

This Eh-vs-pH diagram is calculated for plutonium in water containing hydroxide, carbonate, and fluoride ions. (The ligand concentrations are comparable to those found in water from well J-13 at Yucca Mountain, Nevada, while the plutonium concentration is fixed at 10^{-5} M). Specific complexes form within defined Eh/pH regions, while the stable oxidation states (colors) follow broader trends. For example, more-oxidizing conditions (higher Eh values) stabilize redox-sensitive actinides like plutonium in the higher oxidation states V and VI. The red dots are triple points, where plutonium can exist in three different oxidation states. The range of Eh/pH values found in natural waters is bounded by the solid black outline. In ocean water or in groundwater, plutonium is likely to be found as Pu(IV), while in rainwater or streams, plutonium can assume the V state. Other natural environments will favor Pu(III) or Pu(VI) complexes. The dashed lines define the area of water stability. Above the upper line, water is thermodynamically unstable and is oxidized to oxygen; below the lower line, water is reduced to hydrogen.

Over the course of millennia, however, it is possible that water seeping into a repository will eventually corrode the waste containers. The actinides will then have access to the environment.

Research at Los Alamos has focused on characterizing the behavior of actinides in the environments surrounding those repository sites. (Only small amounts of transuranic elements are generally found in other environments, as discussed in the box "Actinides in Today's Environment" on page 396.)

Our solubility studies, for example, confirm that neptunium is more than a thousand times more soluble in Yucca Mountain waters than plutonium. That is because plutonium in those waters favors the IV oxidation state while neptunium favors the far more soluble V state. Thus, for Yucca Mountain, neptunium is the actinide of primary concern. WIPP, however, is built within a geologically deep salt formation. In the extremely salty brines found there, the focus shifts to plutonium, since

reactions with chloride ions are known to stabilize plutonium in the VI oxidation state. Plutonium(VI) species are much more soluble than Pu(IV) species, and plutonium mobility would be enhanced at WIPP unless a reducing environment can be maintained within or around the waste containers.

Unfortunately, very few studies of actinide geochemistry can be conducted *in situ*, so that we are forced to simulate environmental conditions in the laboratory. The concentrations of the actinides in natural waters are typically on the order of 10^{-6} molar (M) or lower. While those concentrations are high enough to be of environmental concern, they are too low to allow direct study with conventional spectroscopies. We have thus had to adapt advanced spectroscopic techniques, such as x-ray absorption fine structure (XAFS) and laser-induced fluorescence spectroscopies, to study these toxic, radioactive elements.

As an example, recent XAFS investigations of Pu(IV) colloids have yielded significant insights into the colloids' structure, which for years has complicated the determination of Pu(IV) solubility. Scanning electron microscopy (SEM) has helped us elucidate the confusing sorption behavior of U(VI) onto phosphate mineral surfaces. The box on page 412 highlights a few examples of these spectroscopic studies.

The scope of actinide interactions in the environment is too broad to cover in a single article. We will concentrate therefore on the solubility and speciation of actinides in the presence of hydroxide and carbonate ions, which are the two most environmentally relevant ligands. We will then briefly discuss some aspects of actinide sorption and actinide interactions with microorganisms. The solubility and sorption of actinides pose two key natural barriers to actinide transport away from a geologic repository, while microorganisms pose a less-studied but potential third barrier. While we are fully aware of additional geochemical reactions in

3

Table I. Oxidation States of Light Actinides^a

Th	Pa	U	Np	Pu	Am	Cm
III						
IV						
	V	V	V	V	V	
		VI	VI	VI	VI	
			VII	VII		

^aThe environmentally most important oxidation states are bolded.

the environment, such as coprecipitation, mineralization, and diffusion processes (and have thus included them in Figure 1), we will not discuss their roles here.

Oxidation States and Redox Behavior

Water is the dominant transport medium for most elements in the environment. Compared with the pH values and ionic strengths that can be obtained in the laboratory, most natural waters are relatively mild. Typically, they are nearly neutral (pH 5 to 9), with a wide range of redox potentials (from -300 to +500 millivolts) and low salinities (ionic strengths 1 molal). The water conditions determine which actinide oxidation states predominate and which actinide species are stable.

For example, Figure 2 shows the Pourbaix diagram (Eh vs pH) for plutonium in water containing the two most environmentally relevant ligands, the hydroxide (OH⁻) and carbonate (CO₃²⁻) ions. Even in this simple aqueous system, plutonium can exist in four oxidation states: III, IV, V, and VI. (Plutonium is unique in this regard. The Pourbaix diagrams for the other actinides are simpler.) The normal range of natural waters is outlined in the figure and overlaps with the stability fields of plutonium in the III, IV, and V oxidation states. Within this range, plutonium exhibits two triple points,

where species in three different oxidation states are in equilibrium.

Because of intrinsic differences in redox potentials, each actinide will exhibit a different set of oxidation states for a given set of solution conditions. In contrast to plutonium, U(III) is unstable under most conditions and oxidizes easily to U(IV), while U(V) disproportionates easily to U(IV) and U(VI). Neptunium(III) and Np(VI) are on the edges of the water stability region and can exist only under strongly reducing or oxidizing conditions, respectively. Americium and curium will only be found in the III oxidation state under most conditions. Similarly, all actinides beyond curium are dominated by the lanthanide-like trivalent oxidation state.

As a rule of thumb, we expect to find U(VI), Np(V), Pu(IV), Am(III), and Cm(III) as the prevalent oxidation states in most ocean or groundwater environments. But in other aqueous environments, including streams, brines, or bogs, U(IV), Np(IV), and Pu(III, V, VI) are also common and likely to be stable. Table 1 summarizes the oxidation states of the actinides and highlights the environmentally most relevant ones. Some of the states listed in the table, such as Pa(III) or Pu(VII), can be synthesized only under extreme conditions, far from those found in natural systems.

Additional chemical processes occurring in solution are likely to influence the actinide's oxidation state stability.

The stability of Pu(V) in natural waters containing carbonate is an example. The plutonium will complex with the carbonate ligands, and if the plutonium concentration is low (less than about 10⁻⁶ M), radiolytically induced redox reactions are minimized. Consequently, the stability of Pu(V) is enhanced and its disproportionation to Pu(IV) and Pu(VI) is reduced. As discussed later, the solubilities of solids formed from Pu(V) complexes are orders of magnitude greater than those of Pu(IV) solids, so the enhanced stability of Pu(V) would serve to increase the total plutonium concentration in solution.

Another example for the stabilization of actinides in solution is the oxidation of Am(III) and Pu(IV) through radiolytic formation of oxidizing species, such as peroxide (H₂O₂) or hypochlorite (ClO⁻). At high actinide concentrations and hence under the influence of (its own) alpha radiation, those normally stable oxidation states are oxidized to form Am(V) and Pu(VI), respectively, especially in concentrated chloride brines.

Despite the complexity of actinide redox behavior, however, we should emphasize that within a given oxidation state, actinides tend to behave similarly. For example, we can study a U(IV) complex and from it infer the behavior of the analogous Np(IV) and Pu(IV) complexes. In the following discussions, therefore, we often refer to "generic" actinides—e.g., An(IV) complexes—where An is shorthand for actinide.

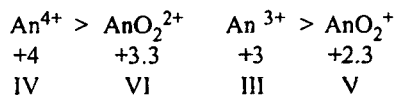
Effective Charge. It has been known for many years that An(IV) forms the strongest, most stable complexes and An(V) the weakest. This behavior follows directly from the effective charges of the ion.

In the III and IV states, the actinides form hydrated An³⁺ and An⁴⁺ ions in solution, respectively. In contrast, the highly charged ions in the V and VI states are unstable in aqueous solution and hydrolyze instantly to form linear *trans*-dioxo cations, AnO₂⁺ and

4

AnO_2^{2+} , with overall charges of +1 and +2, respectively. These cations are often referred to as the actinyl ions.

The covalent bonding between the actinide and the two oxygen atoms in the actinyl ion $(O=An=O)^{n+}$, where $n = 1$ or 2 , enhances the effective charge of the central actinide ion to 2.3 ± 0.2 for AnO_2^+ and 3.3 ± 0.1 for AnO_2^{2+} (Choppin 1983). A ligand approaching the actinyl ion sees this enhanced effective charge and bonds directly to the actinide in the equatorial plane of the linear actinyl ion. Thus, the preference for actinides to form complexes generally follows their effective ion charges, as shown below:



The second and third lines show the ion's effective charge and formal oxidation states.

Recent measurements of bond lengths in the actinyl ions of V and VI complexes reflect the above sequence. A higher effective charge correlates with a stronger, hence shorter, bond to the coordinated ligands. Accordingly, the bond length of the actinyl bonds increases from about 1.75 angstroms (Å) in the VI oxidation state (U=O is 1.76 Å; Pu=O is 1.74 Å) to about 1.83 Å in the V oxidation state (Np=O is 1.85 Å; Pu=O is 1.81 Å).

Because $An(IV)$ has the highest effective charge, it forms the most stable complexes in solution and also forms the most stable precipitates with the lowest solubility. Conversely, $An(V)$ complexes are the weakest, and its solubility-controlling solids are the most soluble. $An(V)$ species are therefore the most likely to migrate through the environment. Table 1 shows that the only transuranics that favor the V state are neptunium and plutonium. But in the environments surrounding repository sites, as well as in most groundwaters and ocean environments, plutonium will most likely assume the IV state. Thus neptunium is predicted to be the most

Actinides in Today's Environment

In 1942, Enrico Fermi built mankind's first fission reactor, and nuclear reactions within that nuclear pile created the transuranic elements neptunium, plutonium, americium, and curium. With the subsequent development of nuclear power, the inventory of transuranics has increased dramatically. As of 1990, the estimated accumulations in spent nuclear fuel were approximately 472 tons of plutonium, 28 tons of neptunium, 6 tons americium, and 1.6 tons of curium.

Fortunately, the amount of radioactive material accidentally released from nuclear power plants has been relatively small. Environmental contamination is severe in only a few locations. Major releases were due to a fire in a reactor at Windscale (now Sellafield) in the United Kingdom in 1957, an explosion at the Kyshtym nuclear waste storage facility in the former USSR in 1957, and an explosion and fire at the Chernobyl reactor in Russia in 1986. In addition, a number of DOE sites in the United States, including the Hanford Site in Washington, Rocky Flats Environmental Technology Site in Colorado, and Idaho National Engineering and Environmental Laboratory in Idaho, contain high local concentrations of actinides.

The main source of transuranics in the environment has been nuclear weapons testing. Since the first detonation of a nuclear device in 1945 at Trinity Site in Alamogordo, New Mexico, more than 4 tonnes of plutonium have been released worldwide (accounting only for announced nuclear tests). Atmospheric and underground tests have also injected about 95 kilograms of americium into the environment, along with tiny amounts of the still heavier element curium.

Until they were banned by international treaty in 1963, aboveground nuclear tests propelled the actinides directly into the atmosphere. There they dispersed and migrated around the globe before settling back to earth. Little can be done to isolate or retrieve this material. It is a permanent, albeit negligible, component of the earth's soils and oceans and poses little health risk to the general public.

Underground nuclear tests injected transuranics into highly localized regions surrounding the detonation sites. These concentrated actinide sources became mineralized and integrated into the rock matrix once their areas cooled and solidified. For the most part, the nuclear material is fixed in place. However, plutonium from a test conducted at the Nevada Test Site in 1968 has been detected in a well more than a kilometer away. Its remarkably fast migration rate (at least 40 meters per year) is likely due to colloidal transport through the highly fractured, water-saturated rock surrounding the detonation site.

soluble and easily transported actinide and is the actinide of major concern in assessing the performance of Yucca Mountain.

Coordination Number and Ionic Radii. Another fundamental aspect about the actinide cations is that they tend to act as hard Pearson "acids," which means that they form strong

complexes with highly anionic ligands by electrostatic interactions. Because the actinide-ligand bond is substantially ionic, the number of bound ligands (the coordination number) and the relative positions of the ligands around the cation are determined primarily by steric and electrostatic principles. Consequently, for a given oxidation state, a range of coordination numbers

5

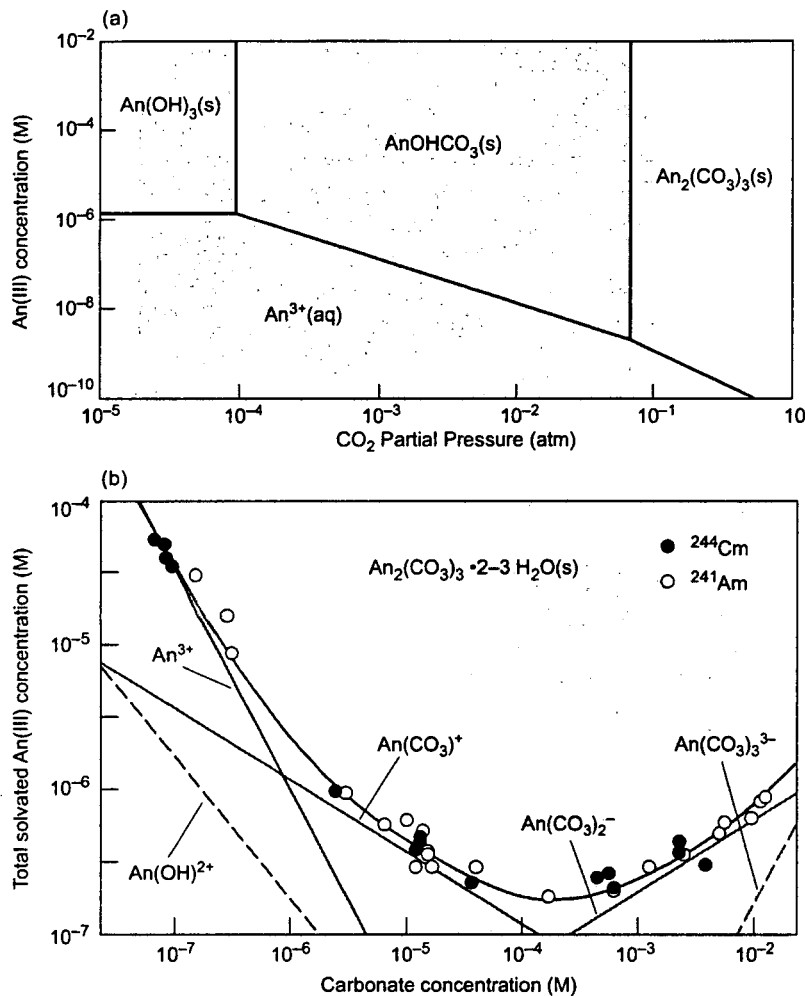


Figure 3. Total An(III) Concentration Versus Carbonate Concentration
 (a) The partial pressure of CO₂ in natural waters spans about three orders of magnitude (gray area). The stability diagram for An(III) solid phases (at pH 7) shows that the An(III) hydroxocarbonate is favored in most natural waters. Lower partial pressures or soluble carbonate concentration translate to increased stability of the An(III) hydroxide; higher pressures mean increased stability for the normal carbonate solids. (b) The red curve is the total concentration of An(III) in solution when the solubility-controlling solid is An₂(CO₃)₃·2-3H₂O(s). Calculated concentrations for individual solution species are indicated by the gray lines that run tangent to the solubility curve, or by the gray dashed lines. At low carbonate concentrations, the An³⁺ ion dominates the solution species. The total An(III) concentration drops rapidly with higher carbonate concentrations as more of the solid phase precipitates. But carbonate complexation begins to stabilize the amount of actinide in solution. By the time the anionic bis- and triscarbonate complexes dominate, the solution concentration increases.

is allowed. Coordination numbers between 6 and 12 have been reported for complexes of An(III) and An(IV) and between 2 and 8 for the actinyl ions.

For example, the aquo ions of the actinides, which have only water molecules in the first coordination sphere surrounding the ion, exhibit coordination numbers that vary with oxidation state: 8-10 for An³⁺, 9-12 for An⁴⁺, 4-5 for AnO₂⁺ and 5-6 for AnO₂²⁺. These coordination numbers have been determined from nuclear magnetic resonance (NMR) and XAFS spectroscopy studies (see the article by Conradson et al. on page 422).

Generally, the stabilities of actinide complexes at a given oxidation state increase with atomic number. This increase in stability follows the trend of the actinide contraction, wherein the

ionic radii decrease with atomic number. The ionic radii for An(IV) ions with coordination numbers of 8 are reported to be 1.00, 0.98, 0.96, 0.95, and 0.95 Å for uranium, neptunium, plutonium, americium, and curium, respectively (Shannon 1976).

Solubility and Speciation

The solubility of an actinide is limited primarily by two properties: the stability of the actinide-bearing solid (the solubility-controlling solid) and the stability of the complexed species in solution. An actinide species will precipitate when its dissolved concentration is above the thermodynamic (equilibrium) solubility of its solubility-controlling solid, or if the kinetics

favors the formation of a solid of higher solubility. Formation of the solid sets an upper concentration limit for the actinide in solution.

Figure 3 illustrates these concepts for An(III), where An is either americium or curium. The data points in the lower graph show the measured total concentration of An(III) in solution. At low pH with increasing carbonate concentration, the hydrated carbonated solid An₂(CO₃)₃·2-3H₂O(s), where (s) indicates the solid phase, readily precipitates and hence lowers the concentration of An³⁺ in solution. But complexation of An³⁺ with carbonate stabilizes the solution species and increases the overall An(III) solubility. As the carbonate concentration increases and the different carbonate species form, the total actinide concentration in solution first

reaches a minimum and then increases due to the formation of anionic An(III) complexes. The solubility would change if conditions favored the formation of a new solubility-controlling solid.

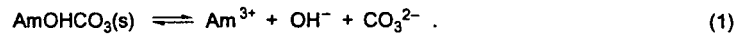
We obtain solubility data by performing experiments in the laboratory under well-controlled conditions in which the actinide concentration is measured while varying the ligand concentration. Such experiments enable us to measure the solubility product K_{sp} and the stability constant β . These thermodynamic parameters are the basis for modeling the solubility boundaries for actinides in natural waters, as discussed in the box on "Solubility and Speciation Parameters."

We should note, however, that meaningful interpretation of solubility data requires a detailed knowledge of the composition, crystallinity, and solubility of the solubility-controlling solid, along with the steady-state concentration and composition of the solution species. Steady state is assumed to be established when the actinide concentration remains stable for several weeks or longer. But the solubility-controlling solids of the actinides generally precipitate as an amorphous phase because radiolysis affects their crystallization. Actinide solids may become less soluble with time as they transform from their initially formed, disordered structures into ordered crystalline solids, thereby lowering their free energy. Such a change, however, may not appear for several years. Thus, the solids formed in laboratory experiments may not represent the most thermodynamically stable solids with the lowest solubility. Laboratory-based solubility studies therefore provide an *upper limit* to actinide concentrations in a potential release scenario from a nuclear waste repository.

Because of their omnipresence, hydroxide ions (OH^-) and carbonate ions (CO_3^{2-}) are the most important ligands that complex to actinides in the environment. While other ligands, such as phosphate, sulfate, and fluoride, can lower the actinide concentration

Solubility and Speciation Parameters

Solubility products (K_{sp}) of actinide-bearing solid phases are indispensable primary data for predicting the concentration limits of actinides in the environment. The solubility product describes the dissolution reaction of the solid into its ionic components. For example, the solubility product of $\text{AmOHCO}_3(\text{s})$, where (s) refers to the solid phase, is given by the product of the concentration of the dissolved ions Am^{3+} , OH^- , and CO_3^{2-} according to the following reaction:



The solubility product is then given by

$$K_{sp} = [\text{Am}^{3+}][\text{OH}^-][\text{CO}_3^{2-}] \quad (2)$$

where the brackets indicate ion concentration. The formation of an actinide complex in solution, for example,



is described by the complex's formation constant, β_n . For the forward reaction in Equation (3), the formation constant is

$$\beta_n = \frac{[\text{Am}(\text{CO}_3)_n^{3-2n}]}{[\text{Am}^{3+}][\text{CO}_3^{2-}]^n} \quad (4)$$

where n refers to the number of ligands. For the reverse reaction, β_n changes sign and is known as the stability constant. The concentration of an actinide solution complex can be calculated by using the known solubility product of the solubility-limiting solid and the formation constant of the species of interest as follows:

$$[\text{Am}(\text{CO}_3)_n^{3-2n}] = \beta_n [\text{Am}^{3+}][\text{CO}_3^{2-}]^n = \beta_n K_{sp} \frac{[\text{CO}_3^{2-}]^{n-1}}{[\text{OH}^-]} \quad (5)$$

Accordingly, the total actinide concentration in solution is given by the sum of the concentrations of species present in solution as follows:

$$\begin{aligned} [\text{Am(III)}] &= [\text{Am}^{3+}] + [\text{Am}(\text{CO}_3)_n^{3-2n}] + [\text{Am}(\text{OH})_m^{3-m}] \\ &= \frac{K_{sp}}{[\text{CO}_3^{2-}][\text{OH}^-]} \times \left(1 + \sum_n \beta_n [\text{CO}_3^{2-}]^n + \sum_m \beta_m [\text{OH}^-]^m \right) \quad (6) \end{aligned}$$

Complexation of the dissolved actinide ion with ligands in solution (large β_n values) generally increases the total actinide concentration in solution.

7

(because of the low solubility of the corresponding solid phase), their concentrations in natural waters are generally low. Consequently, they cannot compete successfully with hydroxide or carbonate complexation. However, organic biodegradation products, such as humates or fulvates, are generally present in natural aquifers and can potentially play a role in actinide solubility and migration.

Hydrolysis. The interaction of actinide and hydroxide ions produces monomeric and—particularly for Pu(IV)—polymeric solution species. The solid-phase structures are oxides, oxyhydroxides, or hydroxides of low solubility.

In the absence of carbonate or other strong ligands (or with very low concentrations of them), trivalent actinides form the positively charged or neutral hydroxo complexes of general formula $An(OH)_m^{3-m}$, where $m = 1, 2, \text{ or } 3$, that is $An(OH)^{2+}$, $An(OH)_2^+$, and $An(OH)_3(aq)$. Similarly, An(IV) forms complexes in solution of general formula $An(OH)_n^{4-n}$, where $n = 1, 2, 3, \text{ or } 4$. The solid hydroxide $An(OH)_n(s)$, where $n = 3$ for An(III) and 4 for An(IV) or the hydrated oxide $AnO_2 \cdot nH_2O$ for An(IV) are expected to control the solubility of actinides in both oxidation states.

Understanding the An(IV) solution chemistry is still a formidable challenge. The high charge allows the An^{4+} ions to easily hydrolyze and form multiple species simultaneously, even at low pH. Plutonium(IV) is known to hydrolyze even in dilute acidic solutions and, at concentrations greater than 10^{-6} M, will undergo oligomerization and polymerization to form very stable intrinsic colloids.

Recent x-ray absorption fine-structure (XAFS) studies, discussed on page 432 in the article by Conradson, have given more insight into the structural details of Pu(IV) colloids. The sub-micron-scale colloid particles are nominally composed of Pu(IV) hydroxo polymers and contain structural characteristics of

plutonium oxide, PuO_2 . However, the XAFS data reveal that these particles possess multiple functional groups, such as terminal hydroxo and bridging oxo and hydroxo groups. Each colloid particle can be considered an amorphous oxyhydroxide compound. The functional groups originate from the polymerization of monomeric species formed through hydrolysis, and the number of functional groups depends on the history of the solution preparation and aging process. While the chemical "structure" of every Pu(IV) colloid may be similar, each colloid can have a unique distribution of functional groups depending on solution preparation, particle size, and water content. Once they form, however, the colloids are inordinately stable in near-neutral solution, presumably because over time, the hydroxo groups that join the plutonium atoms together in the polymer are converted into chemically resistant oxygen bridges.

The generation of Pu(IV) colloids is one of the main processes that complicate determining thermodynamic constants and accurately predicting soluble plutonium concentrations in natural waters. Both the colloids and other amorphous Pu(IV) hydroxide solids span a wide range of structural features, crystallinities, and stabilities, and hence exhibit a wide range of solubilities. The presence of Pu(IV) colloids will therefore complicate any calculation of plutonium solubility, as will be evident when we review plutonium solubility and speciation in Yucca Mountain waters.

Solid hydroxides and oxides are also expected to limit the solubility of An(V) and An(VI) complexes. For example, $Np_2O_5(s)$ has been determined to be the solubility-controlling solid in waters from Yucca Mountain, while schoepite, $UO_2(OH)_2 \cdot nH_2O(s)$ is most stable for U(VI). Interestingly, these solids exhibit both acidic and basic characteristics. With increasing pH, their solubilities tend to decrease in acidic media and increase in alkaline (basic) solutions because of the forma-

tion of anionic hydroxo complexes: $AnO_2(OH)_2^-$ for An(V) and $AnO_2(OH)_n^{2-n}$ ($n = 3$ and 4) for An(VI). The hydrolysis of U(VI) is complicated even more by the formation of polymeric hydroxide species at high U(VI) concentration ($>10^{-5}$ M), i.e., $(UO_2)_3(OH)_5^+$ or $(UO_2)_4(OH)_7^+$. We are currently conducting experiments to see if Pu(VI) undergoes a similar polymerization.

Carbonate Complexation. Carbonate is ubiquitous in nature. In surface waters, such as oceans, lakes, or streams, its concentration ranges generally between 10^{-5} and 10^{-3} M. In groundwaters, its concentration is enhanced (up to 10^{-2} M) because of the increased CO_2 partial pressure, which is about 10^{-2} atm deep underground compared with the atmospheric partial pressure of about 3×10^{-4} atm. These relatively high carbonate concentrations influence the environmental chemistry of actinides in all oxidation states.

Carbonate generally bonds to actinides in a bidentate fashion, that is, two of the three oxygen atoms in the complex bond to the actinide. Thus, actinide carbonate complexes are very strong and highly stable both in solution and in the solid state.

We have investigated the structure of carbonate complexes involving the actinyl ions AnO_2^+ and AnO_2^{2+} . (These complexes are more soluble and thus more easily studied.) As shown in Figure 4, three monomeric solution complexes form. Depending on the solution conditions, these complexes may coexist with each other and with hydroxo complexes. It is therefore difficult to obtain clean, unambiguous structural data about a single species.

We can make inroads into that problem by investigating the stability and structure of the triscarbonato species, $AnO_2(CO_3)_3^{m-6}$, shown in Figure 4(c). This is the limiting (fully coordinated) An(V,VI) carbonate complex in solution. At carbonate concentrations above 10^{-3} M, this complex forms at the exclusion of the others. Using a

battery of spectroscopic techniques, including multinuclear NMR spectroscopy, x-ray diffraction, and XAFS, we have obtained formation constants, bond lengths, and other structural parameters for the An(V) and (VI) carbonate complexes (Clark et al. 1999). This information has helped us understand various aspects of the An(V,VI) carbonate system. (The article by Clark that begins on page 310 describes structural investigations of the Pu(VI) tris-carbonate.)

Carbonate Solids. In many natural waters, carbonate effectively competes with hydrolysis reactions, and mixed hydroxocarbonate solids are likely to form. These solids have general formulas $An(OH)(CO_3)(s)$ for An(III) and $An(OH)_{2m}(CO_3)_n(s)$ for An(IV), where An stands for uranium, neptunium, plutonium, or americium. (The equilibria in these systems are quite complicated, and neither the structure nor the values for n has been determined accurately for An(IV) compounds.)

In the laboratory, however, we can study actinide solids of different compositions by increasing the carbonate concentration. This increase reduces the extent of hydrolysis and allows the formation, for example, of pure An(III) carbonate solids, such as $Am_2(CO_3)_3 \cdot nH_2O(s)$ or $NaAm(CO_3)_2 \cdot nH_2O(s)$, which are the solubility-controlling solids in solutions containing high concentrations of sodium and carbonate. These solids are analogous to the ones formed by the trivalent lanthanides Nd(III) and Eu(III).

Similarly, we have observed the formation of solid An(VI) and An(V) compounds in solutions containing high concentrations of alkali metals and carbonate. These An(V,VI) carbonate solids are inherently interesting. Together, they can be viewed as a structural series, as evident in Figure 5. Binary An(VI) solids have a general composition $AnO_2CO_3(s)$ and are made from highly ordered actinyl carbonate layers. However, An(V) solids need to

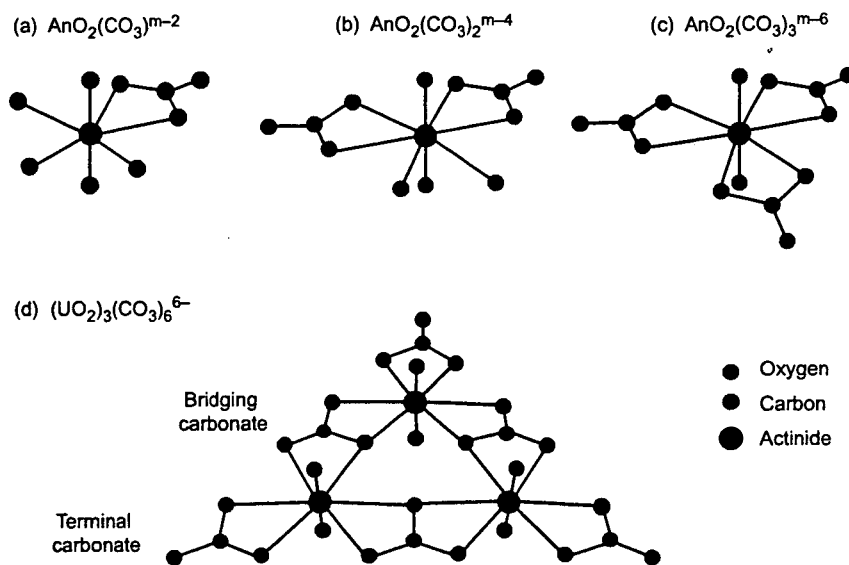


Figure 4. Carbonate Complexes of the Actinyl Ions

Actinides in the V and VI state form similar carbonate complexes in solution, although the charge of the species depends on the oxidation state. Thus, in the three monomeric complexes shown in (a)–(c), $m = 1$ for An(V) and $m = 2$ for An(VI). Actinides in the V state have the lowest effective charge and form the weakest complexes. In these complexes, Np(V) has the longest actinyl bond (An=O) length (1.86 Å). We have also determined only slight changes in the equatorial An–O distances to the carbonate ligands: they vary between 2.42 and 2.44 Å for An(VI) and between 2.48 and 2.53 Å for Np(V). (d) Uranium(VI) may also polymerize at high carbonate and uranium concentrations to form the polynuclear actinyl carbonate complex $(UO_2)_3(CO_3)_6^{6-}$. If present, this polynuclear complex stabilizes U(VI) in solution and increases the overall U(VI) solubility in comparison with the solubility of its monomeric counterpart, $AnO_2(CO_3)_2^{2-}$.

incorporate a monovalent cation, such as Na^+ , K^+ , or NH_4^+ , into their structure (otherwise they would have an overall charge). Thus, we observe only ternary An(V) solids with general compositions $M_{(2n-1)}AnO_2(CO_3)_n \cdot mH_2O(s)$, where $n = 1$ or 2, M is the monovalent cation, and An stands for neptunium, plutonium, or americium.

As the number of cations incorporated into the An(V,VI) carbonate solids increases (stoichiometrically from 0 to 1 to 3), the structures become increasingly open, and the solids generally become more soluble under conditions in which the uncomplexed actinide ion dominates solution speciation. Replacement of the cations with larger ones

enhances the solubility of the actinide by several orders of magnitude. We exploited that fact when we studied the neptunyl “double carbonate” solids $M_3NpO_2(CO_3)_2$. These solids exhibit such low solubilities in near neutral solutions (10^{-4} to 10^{-7} M) that the solution species cannot be studied by many spectroscopic methods. To modify the solubility and obtain more-concentrated neptunyl solutions, we examined the use of large, bulky cations in an attempt to generate an unfavorable fit of the complex into the stable lattices shown in Figures 5(b) and 5(c). We found that tetrabutylammonium provided stable solutions of $NpO_2CO_3^-$ and $NpO_2(CO_3)_2^{3-}$ in

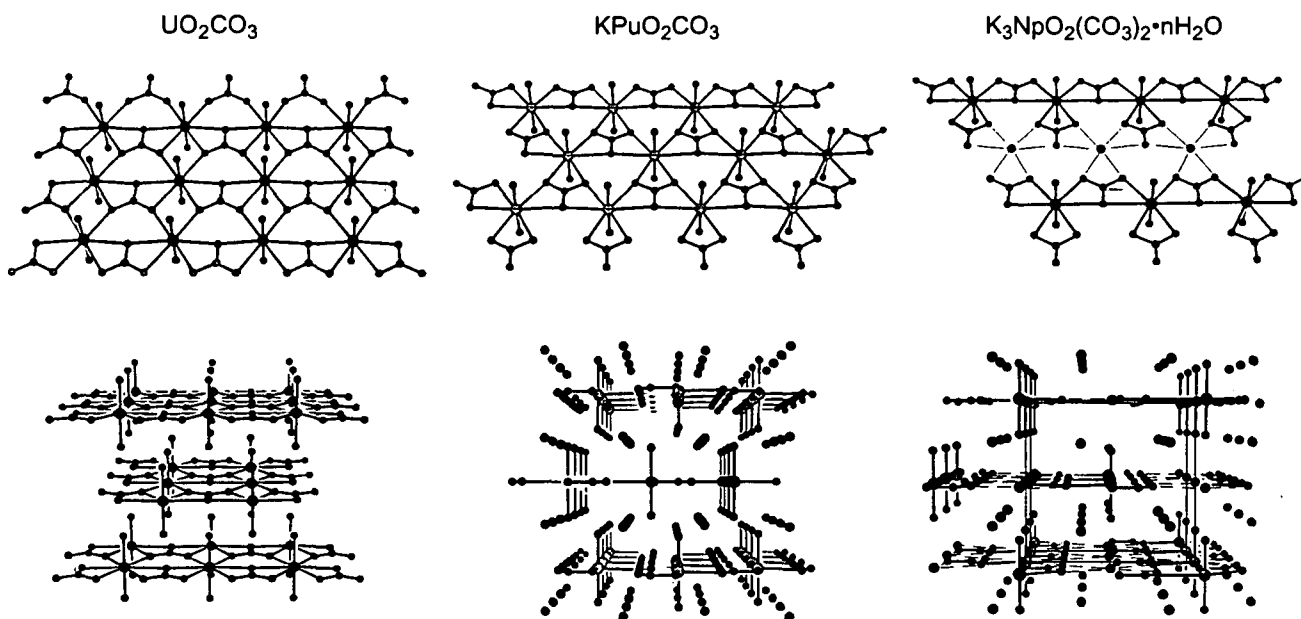


Figure 5. Actinide(V,VI) Alkali Metal/Carbonate Solids

Actinide(V,VI) carbonate solids form a "structural series" that progresses from dense, highly ordered layered structures to more open structures. A single layer is shown above a perspective drawing of each solid. (a) An(VI) will combine with carbonate to form binary solids, such as $\text{UO}_2\text{CO}_3(\text{s})$ or $\text{PuO}_2\text{CO}_3(\text{s})$. Within a layer, each actinide is bonded to two carbonates in a bidentate fashion and to two others in a monodentate fashion. (This is in contrast to solution species, in which carbonate always bonds to an An(VI) in a bidentate fashion.) (b) Actinide(V) ions cannot form binary carbonate solids, since the structural unit would have an overall charge. Solid An(V) carbonates therefore form ternary complexes in conjunction with monovalent metal cations (M), such as Na^+ , K^+ , or NH_4^+ . Within a layer, each actinyl ion binds to three carbonate ligands in a bidentate fashion. The metal ions sit between the layers and form the ternary complex $\text{MAnO}_2\text{CO}_3(\text{s})$. This opens the structure, in comparison with the An(VI) binary-structure, and increases solubility. (c) At higher metal ion concentrations, metal ions will be incorporated into each layer to form very open structures of general formula $\text{M}_3\text{AnO}_2(\text{CO}_3)_2(\text{s})$.

millimolar concentrations over a wide pH range. The enhanced solubility allowed us to study the temperature dependence of the carbonate complexation reactions with near-infrared (NIR) absorption spectroscopy and to obtain additional structural information about the Np(V) solution carbonate complexes with XAFS spectroscopy.

The compositions and stabilities of these actinyl carbonate solids depend on the ionic strength and carbonate concentration and are controlled by the actinide, carbonate, and sodium concentrations in solution. For example, the stability of the Np(V) solids $\text{Na}_{(2n-1)}\text{NpO}_2(\text{CO}_3)_n \cdot m\text{H}_2\text{O}(\text{s})$ is given by the solubility product K_{sp} :

$$K_{\text{sp}} = [\text{Na}^+]^{2n-1} [\text{NpO}_2^+] [\text{CO}_3^{2-}]^n$$

For the An(VI) solid $\text{AnO}_2\text{CO}_3(\text{s})$, n is equal to 1 and its solubility is nominally independent from the sodium concentration in solution. At the low ionic strengths of most natural waters, an unrealistically high NpO_2^+ concentration would be needed to precipitate a ternary Np(V) carbonate solid. Thus, solid An(V) or An(VI) carbonates are in general not observed in natural waters. However, because the ternary compounds of Np(V) have been observed to form in concentrated electrolyte solutions, these solids are important for solubility predictions in brines found at WIPP.

Solubility and Speciation in Yucca Mountain Waters

As a way of tying together many of the concepts presented in the previous sections, we can consider the solubility and speciation of neptunium and plutonium in Yucca Mountain waters. (The article by Eckhardt, starting on page 410, discusses more of the research conducted for Yucca Mountain.) As mentioned earlier, neptunium tends to exist in the V oxidation state in natural waters and because of the lower effective charge of the AnO_2^+ ion, forms weak complexes. Thus, neptunium has the distinction of being the most soluble and transportable actinide and is the

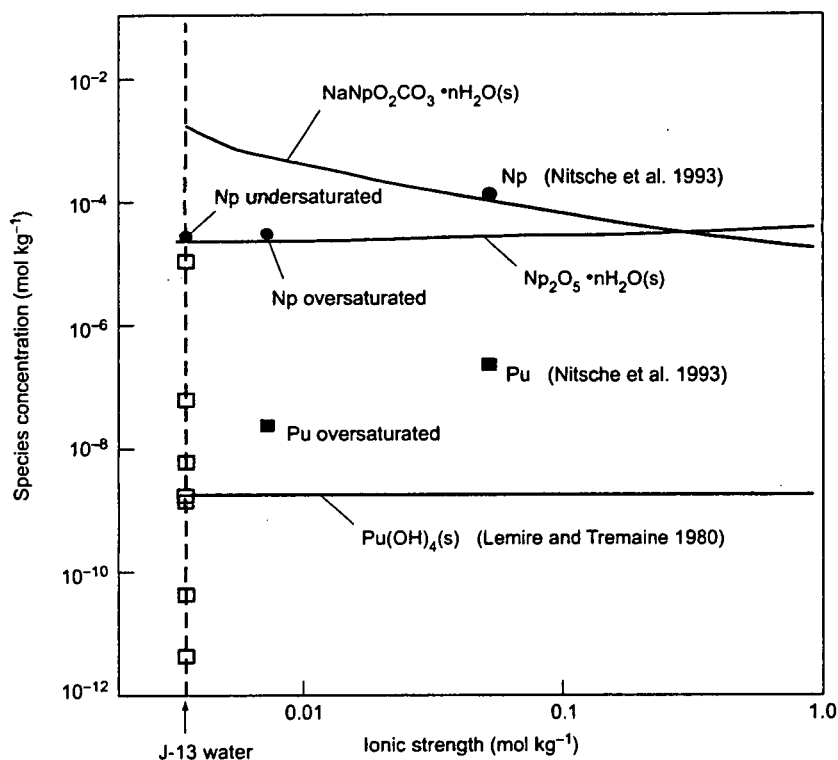


Figure 6. Solubility of Neptunium(V) and Pu(IV) J-13 Water

The figure shows our measured total soluble concentrations of neptunium (red circles) and plutonium (red square) in J-13 water at a fixed carbonate concentration of 2.8 mM (indicated by the dashed line), as well as earlier measurements conducted at a higher ionic strength (black circle and square). The lines are theoretical predictions for different solubility-controlling solids. The Np(V) concentration is about 100 times greater than that of Pu(IV). Our measurements confirm that the controlling Np(V) solid is the oxide $\text{Np}_2\text{O}_5(\text{s})$, rather than the previously postulated sodium carbonate solid $\text{NaNpO}_2\text{CO}_3(\text{s})$. The solubility of plutonium in J-13 water presumably is controlled by amorphous oxides/hydroxides or colloidal forms of Pu(IV), since the measured Pu(IV) solubilities are nearly an order of magnitude higher than predicted by Lemire and Tremaine for the solubility product of $\text{Pu}(\text{OH})_4(\text{s})$. Our data are consistent with the range of Pu(IV) solubilities as calculated from K_{sp} data of Pu(IV) hydroxide or hydrous oxide reported in the open literature (gray area).

one of greatest concern when assessing the environmental safety of the potential underground storage site at Yucca Mountain. Plutonium is considered the most toxic actinide and is always of environmental concern.

Our studies were conducted in water from a particular borehole in Yucca Mountain (J-13 water). The sodium and carbonate concentrations are low (both around 2 to 3 mM), as is the ionic strength of J-13 water (0.003 molal).

However, groundwater conditions within and around Yucca Mountain vary. The carbonate concentration changes (because the CO_2 partial pressure changes with depth), as does the pH, Eh, and temperature. We mimicked this variation in the natural waters by conducting our studies at various pH values while maintaining a constant ionic strength. We also conducted our studies at different temperatures (25°C, 60°C, and 90°C) to approximate the range of

temperatures expected at the repository. Not surprisingly, changing these basic parameters greatly affected the actinide behavior (Eford et al. 1998). Figure 6 summarizes the results of our studies.

The controlling solids for the actinides in J-13 water—in all oxidation states—were mainly oxides and hydroxides. We observed only the formation of greenish brown Np(V) crystalline solids of general formula $\text{Np}_2\text{O}_5 \cdot n\text{H}_2\text{O}(\text{s})$, green Pu(IV) solids of general formula $\text{PuO}_2 \cdot n\text{H}_2\text{O}$ and/or amorphous Pu(IV) hydroxide/colloids. The solubility of neptunium was about 10^{-3} M at pH 6, but dropped to about 5×10^{-6} M at pH 8.5. The neptunium species distribution similarly changed with conditions. At pH 8.5, about 31 percent of Np(V) was present as the neptunyl ion NpO_2^+ . The remaining soluble Np(V) was complexed with either carbonate or hydroxide, with about 58 percent $\text{NpO}_2\text{CO}_3^-$ and 11 percent $\text{NpO}_2\text{OH}(\text{aq})$. At pH 6, however, Np(V) hydrolysis and carbonate complexation reactions were minimized, and all of the neptunium was present as NpO_2^+ .

By comparison, at all pH values examined in our study, 99 percent of the soluble plutonium was calculated to be in the IV state as $\text{Pu}(\text{OH})_4(\text{aq})$. When using $\text{Pu}(\text{OH})_4(\text{s})$ as the solubility-limiting solid in our geochemical models, the plutonium concentration in solution was predicted to be about 10^{-9} M (using the thermodynamic data available in the open literature). As seen in Figure 6, experimental data are about one to two orders of magnitude higher. The discrepancy presumably arises because plutonium solubility is instead controlled by amorphous oxides/hydroxides or colloidal forms of Pu(IV). (Note that if crystalline $\text{PuO}_2(\text{s})$ were the solubility-controlling solid, Pu(IV) solubility would be about 10^{-17} M, well below the Pu(IV) hydroxide solubility range.)

The J-13 water is almost neutral (pH ~7) and has a redox potential of about +430 millivolts. But different water conditions would dramatically affect neptunium solubility, as illustrated

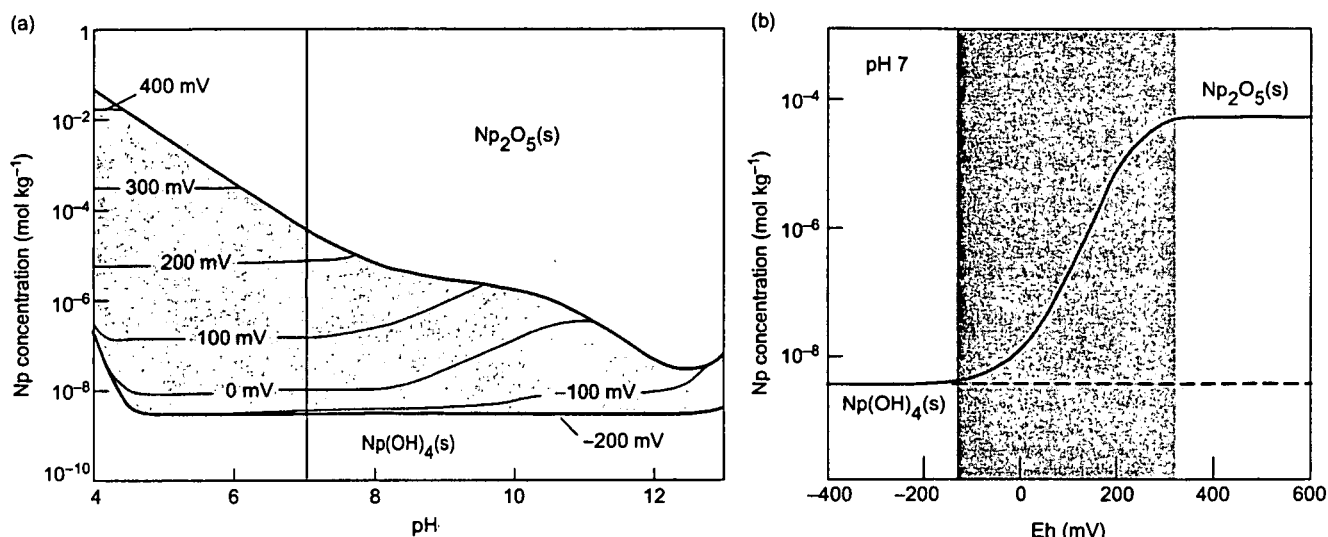


Figure 7. Neptunium Solubility in Yucca Mountain J-13 Water

Neptunium solubility varies tremendously depending on the Eh and pH of the water. (a) The graph shows the neptunium concentration as a function of pH. Calculated solubility boundaries at various Eh values are superimposed on the graph. The colored region contains mainly Np(V) in solution, while the upper and lower bold lines are the solubility boundaries of the Np(V) solid phase, $\text{Np}_2\text{O}_5(\text{s})$, and the Np(IV) solid phase, $\text{Np}(\text{OH})_4(\text{s})$, respectively. Solutions with neptunium concentrations above these boundaries are oversaturated and will precipitate the respective solid. The total neptunium concentration in solution may vary by more than six orders of magnitude over the entire pH range under oxidizing conditions. (b) This graph shows the solubility as a function of Eh at a fixed pH of 7, and corresponds to the Np solubility as one moves along the red line in the previous graph. Under reducing conditions (below -120 mV), Np(IV) dominates the solution speciation. Its concentration in solution is limited to less than 10^{-8} molal by the solubility of $\text{Np}(\text{OH})_4(\text{s})$. As conditions become more oxidizing, Np(V) becomes the redox-stable oxidation state and begins to dominate the speciation. [The Eh determines the Np(IV)/Np(V) ratio in solution, while the overall Np(IV) concentration is maintained by the solubility of $\text{Np}(\text{OH})_4(\text{s})$.] The neptunium concentration rises with redox potential until it reaches approximately 10^{-4} molal at an Eh of -250 mV. Solutions containing a higher neptunium concentration are oversaturated, and the Np(V) solid phase $\text{Np}_2\text{O}_5(\text{s})$ precipitates. The soluble neptunium concentration remains constant from then on. The shaded area spans the region where Eh and solubility of the Np(IV) solid control the neptunium concentration in solution. Outside this area, the solubilities of the Np(IV) and Np(V) solids govern neptunium solution concentration, independent of Eh.

in Figure 7 (Kaszuba and Runde 1999). Under strong reducing conditions (below about -120 millivolts), the total soluble neptunium concentration is limited by a Np(IV) solid phase, $\text{Np}(\text{OH})_4(\text{s})$, and is conservatively assumed to be about 10^{-8} M. Similar to plutonium, the presence of a more ordered solid oxyhydroxide or oxide, such as $\text{NpO}_2(\text{s})$, would reduce that conservative boundary by several orders of magnitude. Under these reducing conditions, Np(IV) also dominates the solution speciation in the form of the neutral complex $\text{Np}(\text{OH})_4(\text{aq})$. The total neptunium concentration will rise as the water conditions become more oxidiz-

ing and Np(V) becomes more stable in solution. Eventually, the Np(V) concentration is great enough to allow a Np(V) solid phase, $\text{Np}_2\text{O}_5(\text{s})$, to precipitate. Formation of this solid sets an upper limit to the soluble neptunium concentration. Within the pH and Eh ranges of most natural aquifers (between 4 and 9 and between -200 and $+700$ millivolts, respectively), that concentration may vary by more than four orders of magnitude.

When modeling actinide release from a radioactive waste repository, we must anticipate the conditions at the source (e.g., close to a spent nuclear fuel container) as well as those in the

far-field environment. Spent nuclear fuel contains mainly UO_2 and actinides in low oxidation states (III and IV). If conditions at the disposal site are reducing—for example, because of microbial activities or the reduction capacity of corroding iron from storage containers—the actinides will be maintained in their lower oxidation states and soluble actinide concentrations may be low. If local reducing conditions change because oxidizing waters infiltrate from the surroundings, actinides will enter their more-soluble oxidation states and begin to migrate into the environment. Once far from the repository, conditions may change drastically,

12

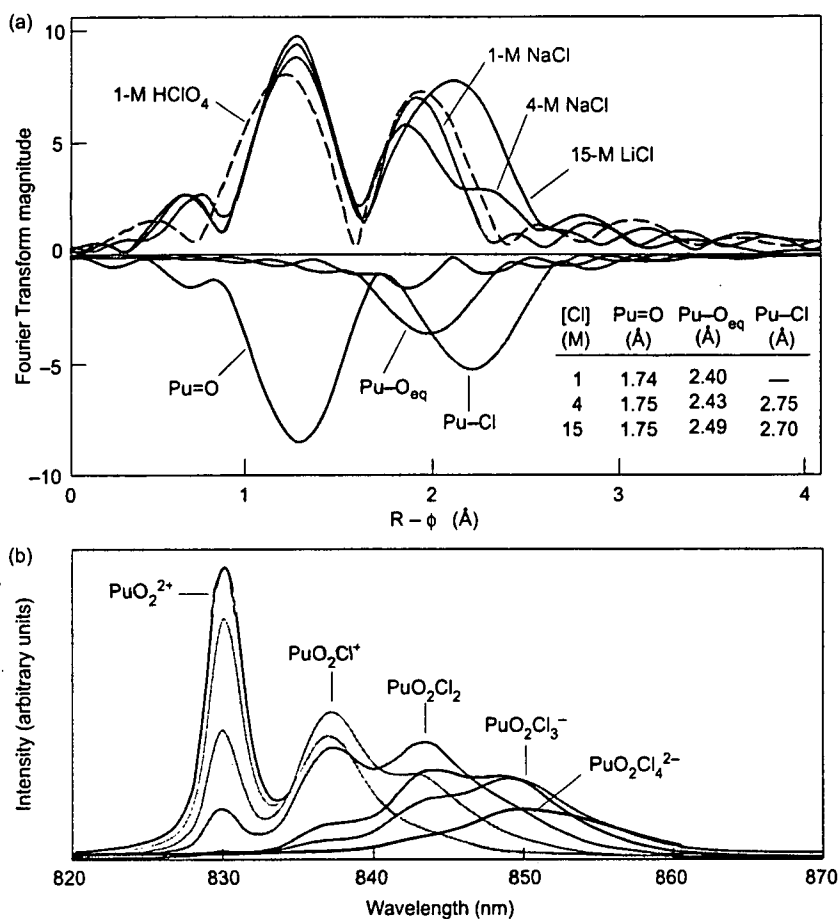


Figure 8. XAFS Data and NIR Spectra of Pu(VI) in NaCl Solutions
 (a) By comparing XAFS data for Pu(VI) in 1-M NaCl, 4-M NaCl, and 15-M LiCl, and non-complexing 1-M HClO₄, we have obtained condition-specific structural information about the solution species. Chloride appears to bond above 1-M chloride in solution. Bonding is clearly evident by 4-M chloride. As seen in the table (inset), the plutonyl bond length (Pu=O) increases slightly after the chlorine bonds and replaces water molecules (indicated by the Pu-O_{eq} bond) in the equatorial plane of the O=Pu=O moiety.
 (b) The absorption bands at 838, 843, 849, and about 855 nm, plus the characteristic band at 830 nm for the PuO₂²⁺ ion, indicate the formation of inner-sphere Pu(VI) chloride complexes. These bands allowed us to determine the formation constant, β , of the most important Pu(VI) chloride complexes in NaCl solutions, PuO₂Cl⁺ and PuO₂Cl₂(aq).

and the transport behavior of redox-sensitive elements such as plutonium or neptunium may change. Clearly, evaluation of actinide mobility in the geochemical environment around nuclear waste repositories must account for soluble actinide concentrations that are controlled by the redox potential of the transport medium and as well by the solubility of the actinides' solid phases.

Complexation with Chloride and Implications for WIPP

In most natural waters, actinides are usually associated with hydroxide or carbonate ligands. However, WIPP, which is designed to hold defense-related transuranic waste, is carved out of a salt formation. Water at the WIPP site thus consists of concentrated brines

that are saturated with chloride salts and exhibit very high ionic strengths (between 4 and 8 molal). With increasing distance from the repository, the brines' ionic strength decreases and may ultimately reach the lower values of most natural surface and groundwaters. This variation complicates our transport models, since the species that form within the WIPP site will not be those that control actinide behavior far from the site.

Chloride has been shown to affect the solubility and speciation of actinide compounds significantly. As mentioned earlier, in most natural waters plutonium favors the IV and V oxidation states, but radiolytic hypochlorite formation in concentrated chloride solution may result in the formation of Pu(VI). Furthermore, complexation by chloride may enhance stabilization of Pu(VI) with respect to reduction to Pu(V) and Pu(IV).

We have studied the complexation reactions of U(VI) and Pu(VI) with chloride using a variety of spectroscopic techniques, including ultraviolet, visible, and NIR absorption and XAFS spectroscopies (Runde et al. 1999). We could determine when U(VI) and Pu(VI) chloride species, such as PuO₂Cl⁺ and PuO₂Cl₂, formed as a function of chloride concentrations (see Figure 8). Interestingly, the tris- and tetrachloro complexes are not formed in significant concentrations in NaCl solutions (up to the point of NaCl saturation). However, we have observed spectroscopically UO₂Cl₄²⁻ and PuO₂Cl₄²⁻ at very high LiCl concentrations and obtained structural data from single crystals synthesized from concentrated chloride solutions.

The interaction of actinides with chloride and other weak anionic ligands significantly affects solubility predictions and must be considered in risk assessments of WIPP and other nuclear waste repositories in salt formations. With regard to neptunium, chloride enhances the Np(V) solubility because of a strong ion interaction between the Np(V) compounds and chloride ions

(see Figure 9). Runde et al. (1996) simulated this interaction using the Pitzer ion-interaction model and developed a Pitzer parameter set to predict the Np(V) solubility at different NaCl concentrations and in artificial brine solutions (Runde et al. 1999). Neglecting the chloride interaction leads to a predicted Np(V) solubility about an order of magnitude too low at a neutral pH. The change of water activity with ionic strength affects the chemical potential of the solid phase because of hydration water molecules in the solid.

Np(V) solubilities were measured from oversaturation in two artificial WIPP brines, AISinR and H-17. The solutions reached a steady state after 241 days. The measured Np(V) solubilities reported in the literature are 2×10^{-6} molal and 1×10^{-6} molal in AISinR and H-17, respectively, while our model predicts Np(V) solubilities of 1×10^{-5} and 3×10^{-6} molal, respectively. The prediction is acceptable for the H-17 brine but lacks accuracy for the AISinR brine. This is because the model accounts only for interactions between Np(V) and Na^+ and Cl^- ions, while the Pitzer parameters for electrolyte ions such as K^+ , Mg^{2+} , Ca^{2+} , and SO_4^{2-} (other constituents in the brines) are unknown. Additional data in various electrolyte solutions are required to develop a more accurate model for the Np(V) solution chemistry in complex brines.

Sorption

The solubility of an actinide species provides an upper limit to the actinide concentration in solution and may be considered as the first barrier to actinide transport. Once an actinide has dissolved in water, its sorption onto the surrounding rock or mineral surfaces is expected to act as a secondary barrier. When the actinide concentrations are far below the solubility limits, as is likely in most surface and groundwater systems, water/rock interfacial processes are

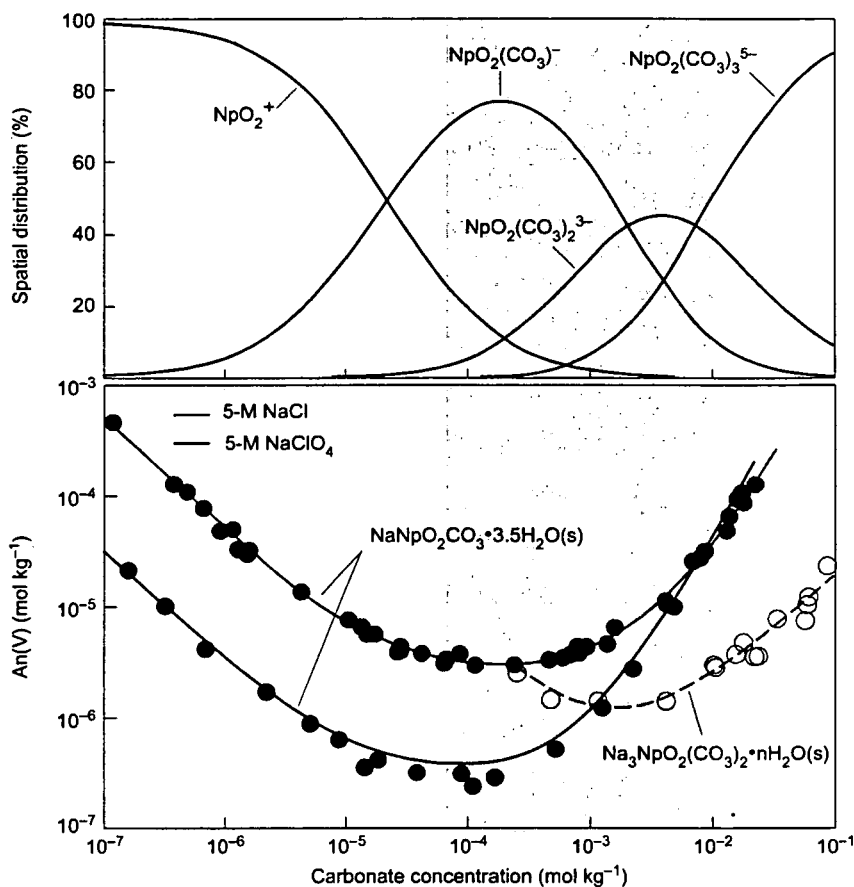


Figure 9. Solubility of Np(V) in Concentrated Electrolyte Solutions

The upper graph shows the distribution of predominant Np(V) solution species as a function of carbonate concentrations, with environmentally relevant concentrations shown in gray. The lower graph shows the soluble Np(V) concentrations in 5-M NaCl solution—conditions that are relevant for WIPP—and noncomplexing 5-M NaClO_4 solution over the same range. Similar data are obtained for Am(V). The neptunium solubility is about an order of magnitude higher in NaCl because of the stabilizing effect of actinide-chloride complexation reactions. The solubility-controlling solid for both curves at low carbonate is the hydrated ternary Np(V) carbonate, $\text{NaNpO}_2\text{CO}_3 \cdot 3.5\text{H}_2\text{O}(\text{s})$. Interestingly, this solid initially forms at high carbonate concentrations. While it is kinetically favored to precipitate, it is thermodynamically unstable. Over time, it transforms to the thermodynamically stable equilibrium phase $\text{Na}_3\text{NpO}_2(\text{CO}_3)_2 \cdot n\text{H}_2\text{O}(\text{s})$ (dashed curve).

expected to dominate actinide transport through the environment. (Simple dilution will lower the actinide concentration, typically to trace concentrations, once the actinide migrates away from the contaminant or waste source.)

Actinide sorption onto mineral surfaces depends on many factors, such as the actinide's speciation and concen-

tration, the flow rate and chemistry of the water, and the composition of the surrounding rocks. In addition, different mechanisms, such as physical adsorption, ion exchange, chemisorption, or even surface precipitation, can fix the actinide to a mineral/rock surface or in general inhibit its transport. Furthermore, redox processes complicate the

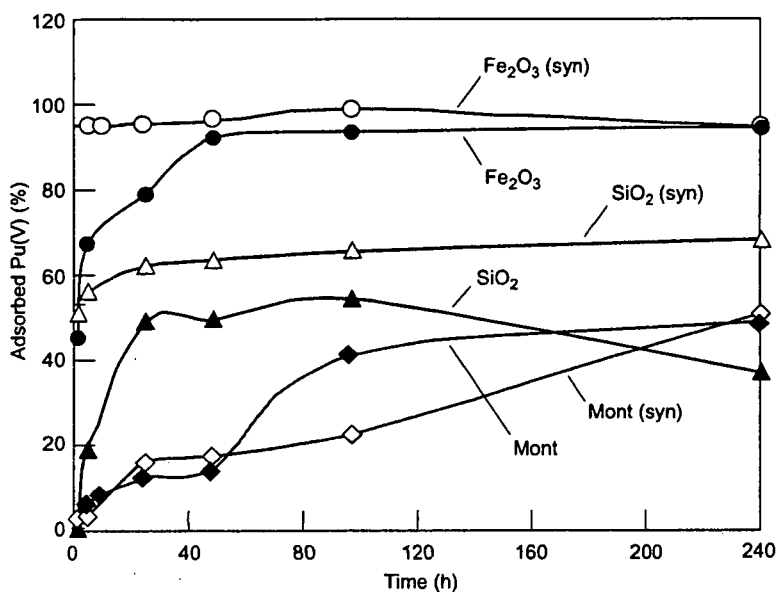


Figure 10. Uptake of Pu(V) by Colloids

Lu et al. (1998) obtained data for Pu(V) adsorption onto colloids, including hematite (Fe_2O_3), silica (SiO_2), and montmorillonite (Mont), in natural J-13 water and in a synthetic (syn) J-13 water. The colloid concentration was maintained at 200 mg/L, with the colloids being about 100 nm in size. The sorption clearly depends on the type of mineral, but the sorption mechanism remains unknown. The time-dependence of the sorption onto montmorillonite suggests a more complicated interaction than occurs with oxide minerals.

Table II. Desorption of Plutonium from Colloids in J-13 Water after 150 Days

Colloid Material	Amount Desorbed	
	Pu(IV) (%)	Pu(V) (%)
Hematite ($\alpha\text{-Fe}_2\text{O}_3$)	0.0	0.01
Goethite ($\alpha\text{-FeOOH}$)	0.57	0.77
Montmorillonite	8.23	0.48
Silica (SiO_2)	19.93	1.04

sorption behavior of neptunium and plutonium. Unfortunately, we are only beginning to understand such actinide sorption and transport mechanisms.

Generally, batch-sorption experiments are performed to investigate how actinides will be retained in the environment. An actinide-containing solution is allowed to come in contact with the geomaterial of interest, and we measure the amount of actinide that

remains in solution. The difference between the remaining and initial actinide concentrations equals the amount that sorbed to the sample. This difference allows us to calculate the batch-sorption distribution coefficient K_d , defined as the moles of radionuclide per gram of solid phase divided by the moles of radionuclide per milliliter of solution and reported as milliliters per gram (mL/g). Low K_d values mean low sorption, and

high values imply effective immobilization due to sorption onto rock surfaces.

Batch-sorption experiments provide helpful information about the sorption capacity of a mineral or soil. But while they are easy to perform, they have some drawbacks. The experiments are fundamentally static and provide only partial information about the dynamic, nonequilibrium processes that occur in nature.² Additionally, the results of batch-sorption experiments are very sample specific and difficult to extrapolate to the different conditions found throughout a repository.

To apply sorption data accurately, we must obtain sorption coefficients from both individual, well-characterized minerals, such as zeolites, manganese oxides, or iron oxyhydroxides, and from mineral mixtures with varying but known compositions. Sorption coefficients from these studies can serve as input data into a transport model that will estimate the actinide retention along water flow paths of known mineral content. The model predictions can then be compared with experimental results obtained from dynamic experiments that use complex soils and rocks.

Studies using minerals (hematite, calcite, gibbsite, albite, and quartz), clays (montmorillonite), and zeolites (clinoptilolite) have shown that Am(III) and Pu(IV) sorb very rapidly to these solids in the following descending order: hematite, montmorillonite, clinoptilolite, and calcite, followed to a much lesser extent by gibbsite, albite, and quartz. But other factors, such as the concentration, solution speciation, and oxidation-state distribution of the actinide species, significantly affect the extent of surface sorption. As an example, K_d values for neptunium sorption onto hematite range from 100 to

²Flow-through, or dynamic, column experiments, wherein the actinide solution is allowed to migrate through a short column of packed geomaterial, provide information about dynamic transport properties. Dynamic column experiments are difficult to perform and interpret, and most of the sorption studies on the actinides are still performed as batch experiments.

15

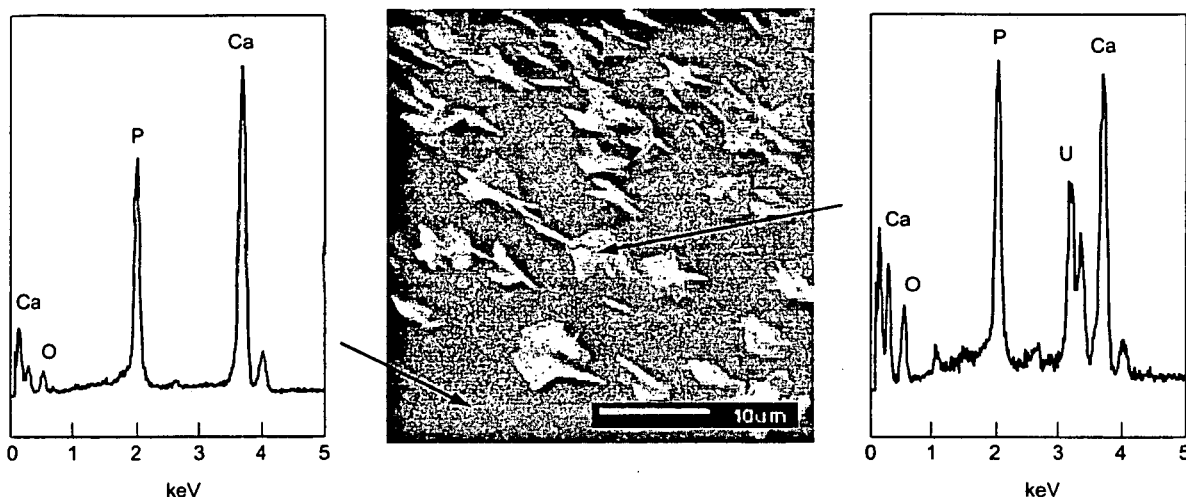


Figure 11. SEM Micrograph of Uranium Precipitate on Apatite

A solution containing U(VI) at 10^{-4} M was kept in contact with apatite for 48 hours. The central SEM micrograph (1100 × magnification) shows crystalline plates on the smooth apatite mineral surface. Analysis of these plates by energy-dispersive spectroscopy (right graph) indicated the presence of calcium, oxygen, uranium, and phosphorus, consistent with crystalline uranium phosphate. Similar analysis of the bare regions of apatite (left graph) showed signals corresponding to only calcium, oxygen, and phosphorus. The precipitates were observed at uranium concentrations above 10^{-5} M. Studies show that at lower concentrations, uranium sorbs, rather than precipitates, to the mineral surface.

2000 mL/g, while plutonium sorption onto hematite results in K_d values above 10,000 mL/g. This difference is mainly caused by the different stabilities of the actinide oxidation states and their complexation strengths. The low charge of the NpO_2^+ ion results in a low sorption of neptunium, while Pu(IV) dominates the complexation and sorption processes of plutonium. Plutonium(V) is expected to follow the low sorption affinity of Np(V).

Lu et al. (1998) determined the sorption of Pu(V) onto oxide and clay colloids (Figure 10). Sorption onto iron oxides, such as hematite, is strong and irreversible, but only 50 percent of the Pu(V) is sorbed on the montmorillonite (clay). However, the sorption mechanisms are largely unknown. The time-dependence of the sorption onto the clay suggests a more complicated interaction than occurs with oxide minerals.

Interestingly, the *desorption* of Pu(V) does not follow this general pattern. Lu et al. (1998) also discussed the desorption of Pu(IV) and Pu(V) from various colloids. Table II summarizes

their findings: Surprisingly, Pu(IV) exhibits a greater tendency to desorb than Pu(V). Particularly striking is the relatively high desorption of Pu(IV) from silica, which indicates a different sorption mechanism or different binding to the silica functional groups than to the Fe(III) minerals, including possible changes in plutonium oxidation states.

These investigations indicate the importance of understanding the oxidation-state stability of the actinide sorbed on a mineral surface. Redox-active minerals, such as manganese or iron oxide/hydroxides, are present in subsurface environments and may alter the redox states of uranium, neptunium, and plutonium. At the Rocky Flats Environmental Technology Site, seasonal variations of plutonium concentrations in settling ponds correlate astonishingly well with soluble manganese concentrations, indicating a potential release of plutonium by way of seasonal redox cycling.

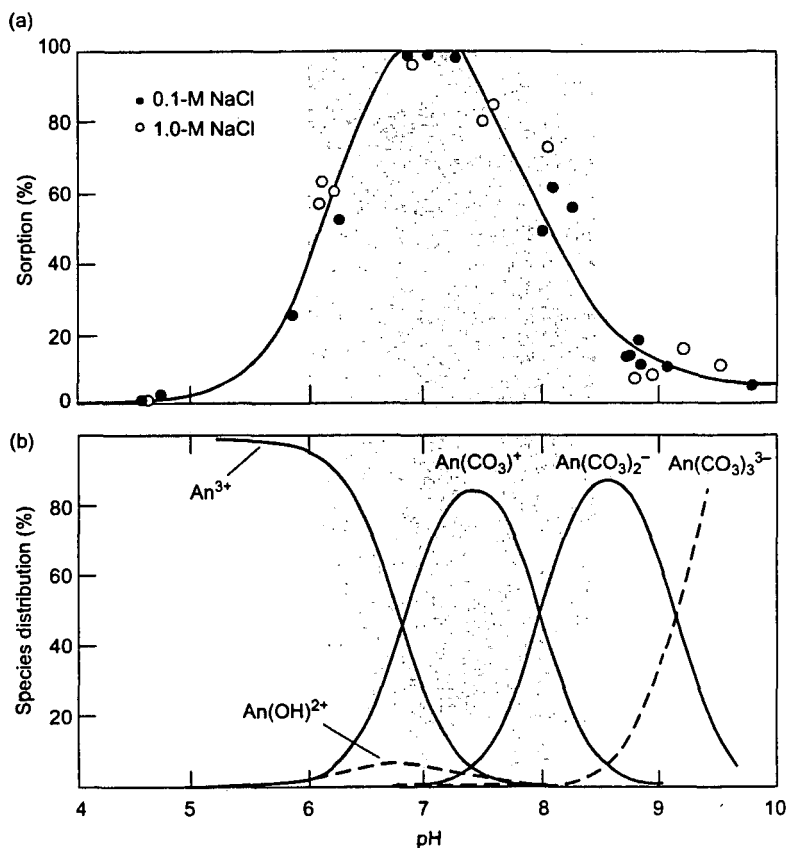
It has been generally hypothesized that the environmentally mobile Pu(V)

is reduced to Pu(IV) through the formation of strong mineral-surface complexes. Quite surprisingly, Neu et al. (2000) showed that Pu(V) is not reduced when sorbed on MnO_2 . X-ray absorption near-edge structure indicated the presence of Pu(V) on MnO_2 , even though the starting material of the batch-sorption experiment was colloidal Pu(IV) hydroxide. Their data also indicated that the plutonium was oxidized to Pu(VI). The only time they did not observe the higher-oxidation-state surface species was when Pu(IV) was complexed with a strong ligand, such as nitrilo triacetic acid (NTA). These observations strongly support the hypothesis that plutonium undergoes a redox cycling that is enhanced by surface interactions. We need more data about the surface species, however, to model such interactions.

Obviously, batch experiments alone cannot elucidate sorption mechanisms. Specifically, we have to distinguish between surface precipitation and interfacial molecular reactions in order to model sorption behavior. In the event

Figure 12. Correlation between An(III) Solution Speciation and Sorption onto Montmorillonite

(a) Even with an order-of-magnitude difference in NaCl concentration, sorption of the trivalent actinides Am(III) and Cm(III) peaks in near-neutral waters. At lower pH, the An^{3+} ion is stable and does not participate in complexation reactions with the most common ligands, hydroxide or carbonate, no matter if the ligands are in solution or on a surface. At higher pH, negatively charged An(III) species are formed that increase the species' solubility and reduce their sorption because they are repelled from the negatively charged functional groups on the mineral surface. (b) Calculations for a weak sodium chloride solution (0.1-M NaCl and CO_2 partial pressure of 0.01 atm) suggest that sorption is mainly correlated with the presence of cationic solution species. The gray area denotes the pH range of natural waters.



of a surface precipitation, the K_d value may represent the solubility product of the surface precipitate but will not reflect the sorption behavior of an actinide species.

For example, phosphate-containing minerals, such as apatite, are known to reduce thorium and uranium concentrations in contaminated solutions. Sorption distribution coefficients for U(VI) and Th(IV) have been reported in the literature, but there are also reports of U(VI) and Th(IV) precipitates. Our SEM studies have identified microcrystalline precipitates on the apatite when the initial U(VI) concentrations were above 10^{-5} M (see Figure 11). At lower U(VI) concentrations, no surface precipitation was observed. Thus, at the higher concentrations, the K_d values actually reflect a solubility product, while at the lower concentrations, the decrease of U(VI) in solution results from sorption of the actinide onto the mineral surface.

Complexation reactions can influ-

ence the actinide sorption processes that also depend strongly on pH (Figure 12). For the trivalent actinides Am(III) and Cm(III), the sorption reaches a peak under conditions of near-neutral waters. There, the cationic An(III) solution species predominate solution speciation. At lower pH, the An^{3+} ion is stable and does not participate in bonding with hydroxide or carbonate ligands. At higher pH, negatively charged An(III) species are formed that exhibit reduced interactions with chemically active groups at the mineral surface. Mineral or rock surfaces at high pH are generally negatively charged, and apparently the negatively charged actinide species are repelled from the anionic surface groups. As such, anionic actinide species behave as simple anionic ligands, such as SO_4^{2-} , CrO_4^{2-} or AsO_4^{3-} . In addition to An(III) species, the same trend of enhanced stability and low surface retention has been observed for the An(VI) complex $UO_2(CO_3)_3^{4-}$.

Enhanced modeling efforts have

begun to address the fundamental mechanism of actinide adsorption onto mineral surfaces. Janecky and Sattelberger (unpublished results) modeled the adsorption behavior of Np(V) on calcite by minimizing the free energy of the coordination. The structural parameters of $NpO_2CO_3^-$, which is the main solution complex in neutral and low-carbonate waters (such as J-13 water), were used to mimic the adsorption. The resulting surface-complex modeling indicates a distance of about 4 Å between the neptunium center and the nearest calcium ions in the calcite structure. Data from preliminary XAFS studies support this distance. Although this agreement between experiment and theory is encouraging, more detailed studies have to be performed to develop much more accurate transport models, including this surface complexation model.

We are also trying to better understand the sorption/desorption reactions of actinides with colloids and the

17

actinides' resulting transport characteristics. This area of environmental migration received heightened attention with the discovery of plutonium in a borehole at the Nevada Test Site (Kersting et al. 1999). The plutonium had evidently migrated 1.3 kilometers in only 30 years. (Each nuclear test is characterized by a unique $^{239}\text{Pu}/^{240}\text{Pu}$ isotope ratio, and that ratio can be used to identify the plutonium source.) As discussed in the article by Maureen McGraw, we now believe that colloidal transport was responsible for this remarkably fast movement of plutonium through the water-saturated rock. It is not clear, however, whether the transport was facilitated by intrinsic plutonium colloids or natural (clay or zeolite) colloids. What is clear is that transport models to date have underestimated the extent of colloidal transport on plutonium mobility.

Microbial Interactions

We have discussed the most prominent chemical processes involving actinides in the environment: dissolution and precipitation of solids, complexation in solution, and sorption onto surfaces. But there is growing attention to the importance of actinide interactions with microorganisms. Great varieties of microorganisms exist in all aquifers and soils, and many survive under the most extreme conditions, such as around hydrothermal vents at the bottom of the ocean, within deep subterranean aquifers, or within the hypersalinity of geologic salt beds.

Microorganisms can accumulate on solid surfaces often via formation of biofilms, or they may be suspended in the aquifer. As such they act as mobile or even self-propelled colloids. The concern is that the actinides can be associated with microbes, either through surface binding or through metabolic uptake, and be transported by them through the environment. However, the microorganisms' role in environmental transport behavior of radioactive

contaminants is still virtually unknown.

Microorganisms, especially bacteria, are also known to mediate redox processes. They may reduce elements from higher oxidation states and use the enthalpy of the redox reaction to grow and reproduce. Through metabolic activity, microbes can also establish reducing conditions by changing the pH and Eh of the local waters. While direct experimental evidence is still lacking, it is almost certain that some microbes can catalyze the transformation of uranium, neptunium, and plutonium into less-soluble forms. Several bacteria species have been reported in the literature to effectively reduce the highly mobile U(VI) into the far less soluble and mobile U(IV).

Given these characteristics, microbes could pose a third natural barrier to actinide transport from geologic repositories and could also help remediate actinide-contaminated soil, groundwater, and waste streams. The ultimate goal is to use microorganisms as "living" backfill to immobilize actinides through processes such as bioreduction, biosorption, or bioprecipitation and mineralization. At this time, however, actual applications of bacteria in remediation strategies and field demonstrations are rare.

Recent WIPP-related studies at Los Alamos have focused on the interaction of uranium and plutonium with the bacteria's cell walls or byproducts, such as extracellular biopolymers, and the toxicity and viability of microorganisms in the presence of the actinides. Francis et al. (1998) have shown that actinides are associated only at low levels with the halophilic bacteria isolated from muck pile salts around the WIPP site. The extent of association varied with bacterial culture, actinide species, pH, and the presence of organic or inorganic complexants. The radiolytic effects on the microbial viability were found to be negligible.

However, other microorganisms can concentrate metal ions to a great extent. Hersman et al. (1993) observed a strong uptake of plutonium by *pseudomonas*

sp. Within the first week of the experiment, the bacteria concentrated plutonium to levels that were nearly 10,000 times greater than a sterile control organism. Lower uptake was observed for contact times of two weeks or longer. Another strain of this bacteria, *pseudomonas mendocina*, is known to remove lead from Fe(III) hydroxide/oxides and was investigated for its potential to remove radionuclides from those environmentally abundant minerals. In fact, Kraemer et al. (2000) found that 20 percent of the sorbed plutonium was removed by this aerobically growing bacteria after about four days. The experimental conditions are presently optimized to remove the majority of the sorbed plutonium and to maximize its potential application in soil remediation strategies.

Leonard et al. (1999) also studied the inhibitory and toxic effects of magnesium oxide, MgO, on these WIPP-derived bacterial cultures. Magnesium oxide is of specific interest because it was chosen as backfill material at the WIPP repository to maintain the pH between 9 and 10, to reduce the amount of infiltrating water, and to limit the amount of CO₂ that can accumulate through degradation of cellulose and other organic compounds in the wastes. Initial studies indicated an inhibited cell growth as the amount of MgO increased, as well as a decrease in microbially generated gas (N₂O) by active halophilic bacteria. Ultimately, the toxic effect of MgO inhibits microbial growth, and consequently microorganisms may be unable to create a reducing environment at the repository that would stabilize actinides.

A more detailed study on the microbial association mechanism included analysis of the uptake of uranium and plutonium by sequestering agents and extracellular polymers (exopolymers). As an example, some exopolymers produced by *bacillus licheniformis* consist of repeating γ -polyglutamic acid (γ -PGA). Neu et al. (manuscript in preparation) observed actinide hydroxide precipitation at metal-to-glutamate ratios

higher than 1:20, but both U(VI) and Pu(IV) ions formed soluble complexes at ratios 1:100 and 1:200, respectively. Presumably at the higher PGA concentrations, the actinide ion is encapsulated and isolated from hydroxo-colloid formation. The binding strength for U(VI) and Pu(IV) is lower than for other strong ligands and chelators, such as Tiron or NTA, but on the same order as for other exopolymers or humic acids.

An upper binding boundary for the polyglutamate exopolymer was determined to be about 0.5 micromoles Pu(IV) per milligram of γ -PGA. Active cells of *bacillus licheniformis* bonded to more than 90 percent of the introduced Pu(IV)—up to 8.4 micromoles of Pu(IV) were added. As expected, other functional groups on the exterior cell surface (in addition to the PGA exopolymer) increase the number of binding sites and enhance metal binding.

This research clearly shows that actinides bind with microorganisms and their metabolic byproducts. Depending on the static or dynamic nature of the microorganism, the interaction of plutonium and other actinides with extracellular ligands may affect the actinides' mobility both away from storage containers and within the environment. Future studies will focus on understanding the mechanisms of actinide/microbial interactions and exploiting their potential for remediation and immobilization efforts. Uptake studies of plutonium by means of sequestering agents are highlighted in the box on "Siderophore-Mediated Microbial Uptake of Plutonium" on page 416.

Concluding Remarks

From this overview of actinide interactions in the environment, it should be clear that such interactions are complex. Each local environment is unique, and the site-specific conditions determine which actinide species predominate as well as each species' overall transport and migration characteristics.

In general, actinide solubilities are low in most natural waters—below micromolar concentrations. Actinides in the V oxidation state will have the highest solubilities; those in the IV oxidation state, the lowest. Conversely, An(V) species show low sorption onto mineral and rock surfaces, and An(IV) species tend to sorb strongly. Typically, neptunium is the only actinide that favors the V oxidation state, and as such it is the most soluble and most easily transportable actinide under environmental conditions. Plutonium favors the IV oxidation state in many natural waters, and normally its solubility is quite low. Once plutonium is in solution, its migration is dominated by a variety of processes, including redox reactions in solution or on mineral surfaces, sorption, colloidal transport, simple diffusion into rock interfaces, coprecipitation, and mineralization. Furthermore, increasing research activities indicated that microbes can affect actinide migration, either through direct association or by helping to maintain a reducing environment.

To understand this complex set of interacting processes requires that we have a strong, multidisciplinary foundation in environmental chemistry, molecular science, and interfacial science and the requisite spectroscopies, subsurface testing, and laboratory experiments. But we also need to interpret experimental results within the context of the multi-component natural system.

A case in point is the recent identification of a higher oxide of plutonium of general formula $\text{PuO}_{2+x}(\text{s})$, which is formed by water-catalyzed oxidation of $\text{PuO}_2(\text{s})$. As discussed by Haschke in the article beginning on page 204, this Pu(IV) "superoxide" may also contain Pu(VI), which would increase plutonium solubility. In a recently published paper (Haschke et al. 2000), the authors speculated that the Pu(VI) could dissolve and be transported more easily from a nuclear waste storage site than previously estimated. Further, they conjectured that Pu(VI) might have caused the rapid migration of plutonium

at the Nevada Test Site. In these speculations, however, they failed to include influential environmental factors.

While we acknowledge that the potential presence of Pu(VI) in a $\text{PuO}_2(\text{s})$ matrix may increase the dissolution kinetics, the chemical conditions of the local environment (water and rock compositions) determine the stability of plutonium oxidation states in the aqueous phase and the overall plutonium mobility. Under ambient conditions and in most aqueous environments, Pu(VI) is unlikely to be stable. Once in solution, it is typically reduced to lower oxidation states and, depending on the water redox potential, may eventually precipitate as $\text{Pu}(\text{OH})_4(\text{s})$ or $\text{PuO}_2(\text{s})$. Consequently, the fact that the superoxide $\text{PuO}_{2+x}(\text{s})$ may include Pu(VI) does not automatically imply enhanced plutonium solubility or mobility in the natural environment. Furthermore, given the results on colloidal transport, it is improbable that Pu(VI) is responsible for the plutonium migration at the Nevada Test Site.

As the inventory of actinides in interim storage facilities grows and storage containers age, increasing the risk of accidental releases, and as the safety of permanently storing nuclear waste in geologic repositories must be evaluated, it becomes increasingly important to understand how actinides will interact with the environment. More sophisticated models are needed to account for all the potential migration paths away from an actinide source. Theoretical and experimental scientists will be challenged for years by the demands of developing those models. ■

Further Reading

- Brown, G. E., V. E. Heinrich, W. H. Casey, D. L. Clark, C. Eggleston, A. Felmy, D. W. Goodman, et al. 1999. *Chem. Rev.* 99: 77-174.
- Clark, D. L., S. D. Conradson, D. W. Keogh, M. P. Neu, P. D. Palmer, W. Runde, et al. 1999. X-Ray Absorption and Diffraction Studies of Monomeric Actinide Tetra-, Penta-, and Hexavalent Carbonato Complexes. In *Speciation, Techniques and Facilities for Radioactive Materials at Synchrotron Light Sources*, OECD Nucl. Energy Agency. 121.
- Choppin, G. R., and E. N. Rizkalla. 1994. Solution Chemistry of Actinides and Lanthanides. In *Handbook on the Physics and Chemistry of Rare Earths*. Edited by K. A. Gschneidner Jr. and L. Eyring. New York: North-Holland Publishing Co.
- Choppin, G. R., J.-O. Liljenzin, and J. Rydberg. 1995. Behavior of Radionuclides in the Environment. In *Radiochemistry and Nuclear Chemistry*. Oxford: Butterworth-Heinemann.
- Choppin, G. R., 1983. *Radiochim. Acta* 32: 43.
- Dozol, M., R. Hagemann, D. C. Hoffman, J. P. Adloff, H. R. Vongunten, J. Foos, et al. 1993. *Pure and Appl. Chem.* 65: 1081.
- Efurd, D. W., W. Runde, J. C. Banar, D. R. Janecky, J. P. Kaszuba, P. D. Palmer, et al. 1998. *Environ. Sci. Tech.* 32: 3893.
- Francis, A. J., J. B. Gillow, C. J. Dodge, M. Dunn, K. Mantione, B. A. Strietelmeier, et al. 1998. *Radiochim. Acta* 82: 347.
- Hascke, J., T. Allen, and L. Morales. 2000. *Science* 287: 285.
- Hersman, L.E., P. D. Palmer, and D. E. Hobart. 1993. *Mater. Res. Soc. Proc.* 294: 765.
- Kraemer, S. M., S. F. Cheah, R. Zapf, J. Xu, K. N. Raymond, and G. Sposito. 2000. *Geochim. Cosmochim. Acta* (accepted).
- Kazuba, J. P., and Runde, W. 1999. *Environ. Sci. Tech.* 33: 4427.
- Kersting, A. B., D. W. Efurd, D. L. Finnegan, D. J. Rokop, D. K. Smith, J. L. Thompson. 1999 *Nature* 397: 56.
- Kim, J. I. 1986. Chemical Behavior of Transuranic Elements in Natural Aquatic Systems. In *Handbook on the Physics and Chemistry of the Actinides*. Edited by A. J. Freeman and G. H. Lander. New York: North-Holland Publishing Co.
- Langmuir, D. 1997. Chap. 13. In *Aqueous Environmental Geochemistry*. Upper Saddle River, NJ: Prentice Hall.
- Leonard, P. A., B. A. Strietelmeier, L. Pansoy-Hjelvik, R. Villarreal. 1999. Microbial Characterization for the Source-Term Waste Test Program (STTP) at Los Alamos. Conference on Waste Management 99, Tucson, AZ.
- Lemire, R. J. and P. R. Tremaine. 1980. *J. Chem. Eng. Data.* 25: 361.
- Lu, N., I. R. Triay, C. R. Cotter, H. D. Kitten, and J. Bentley. 1998. "Reversibility of sorption of plutonium-239 onto colloids of iron oxides, clay and silica." Abstract of Agronomy, p.31 ASA, CAA, SSSA Annual Meetings, Baltimore, MD.
- Neu, M. P., W. Runde, D. M. Smith, S. D. Conradson, M. R. Liu, D. R. Janecky, and D. W. Efurd. 2000. EMSP Workshop, Atlanta, GA.
- Nitsche, H., A. Muller, E. M. Standifer, R. S. Deinhammer, K. Becraft, T. Prussin, R. C. Gatti. 1993. *Radiochim. Acta.* 62: 105.
- Runde, W., S. D. Reilly, M. P. Neu. 1999. *Geochim. Cosmochim. Acta.* : 3443.
- Runde, W., M. P. Neu, D. L. Clark. 1996. *Geochim. Cosmochim. Acta* 60: 2065.
- Shannon, R. D. 1976. *Acta Cryst.* 32A: 751.

Wolfgang Runde earned B.S. and Ph.D. degrees in chemistry from the Technical University of Munich, Germany, in 1990 and 1993, under the direction of Professor Dr. J. I. Kim. He then worked for two years as a scientific staff



member at the Institute for Radiochemistry, TU Munich. During this time, he was invited to work as a guest scientist at Sandia National Laboratories on technical aspects of the actinide source term

model for WIPP. Wolfgang then spent a year as postdoctoral fellow at the G. T. Seaborg Institute for Transactinium Science at the Lawrence Livermore National Laboratory before joining the Chemical Science and Technology Division at Los Alamos National Laboratory in 1996. He is presently a staff member and leader of the Actinide Environmental Chemistry team in the Environmental Science and Waste Technology Division with a joint appointment in the Nuclear and Radiochemistry group in the Chemical Science and Technology Division. His research interests are in the areas of inorganic, environmental, and radiochemistry of f elements, including the actinides, with the focus on nuclear waste isolation and the environment. His research activities have been closely affiliated with the national nuclear waste programs in the US (WIPP and Yucca Mountain) and Germany (Gorleben).

Spectroscopies for Environmental Studies of Actinide Species

Wolfgang Runde

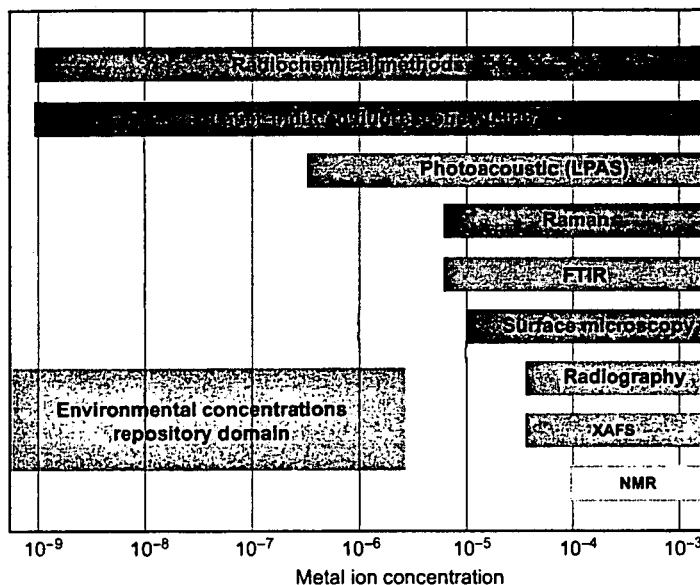


Figure 1. Spectroscopic Sensitivities

In order to understand the complex chemistry of actinides in the environment, we need to have detailed information about its chemical speciation in natural waters in association with natural mineral phases. Chemical speciation identifies not only the molecular formula, charge, and structure of an element's compounds, but also the isotopic composition of the molecule and the oxidation states of its constituents. This information is a prerequisite for making accurate assessments of the compound's thermodynamic and kinetic stability.

Unfortunately, actinide solubilities in natural waters are expected to be generally below micromolar (10^{-6}) concentrations, and these low concentrations complicate a direct non-destructive investigation. A number of spectroscopic methods have been developed to optimize understanding and quantification of actinides' reactions on the molecular scale (see Figure 1). Because of differences in the physical properties among the actinides, no single spectroscopy can adequately probe all actinides. We have had to apply a range of spectroscopic techniques in order to gain maximum insight into the environmental chemistry of the actinides. Some examples of our multifaceted approach to studying solid-state and solution speciation are given below. Other examples are given in the main text.

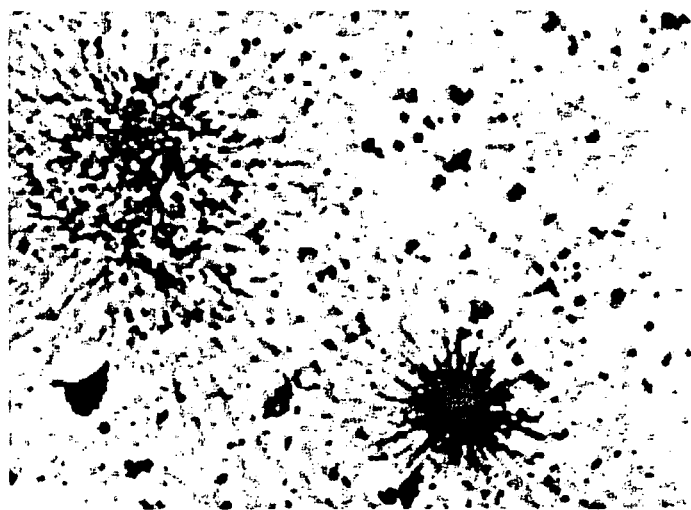


Figure 2. Autoradiograph of Plutonium in Rocky Flats Soil

Autoradiography. Autoradiography is one of the oldest techniques in radiochemistry, having been pioneered by Becquerel in 1896. It uses photographic emulsions to detect and determine the distribution of radioactive material in media and on surfaces. While used extensively for medical and biological research, the technique can also provide qualitative visual information on the distribution and density of radioactive material in soil. The photo seen in Figure 2 is a microautoradiograph of a 3.5 mm x 4.5 mm soil sample from the Rocky Flats Environmental Technology Site. The sample is contaminated with plutonium and americium, and alpha particles emitted by either of those radioactive elements leave omni-directional tracks in the emulsion. We used this visualization technique to separate and concentrate 'hot' soil particles for further spectroscopic analysis. XAFS spectroscopy and SEM/EDS (see below) identified plutonium as the major contaminant in the soil, which contained only minor amounts of americium.

21

Scanning Electron Microscopy (SEM) and X-Ray Photoelectron Spectroscopy (XPS). The interaction of actinides with mineral surfaces have been studied by radiochemical techniques (isotherm tracer experiments) or spectroscopic techniques. SEM and XPS are two surface analysis techniques that are widely used to investigate speciation at a solid-liquid interface. We use SEM to examine the crystallinity of micron-scale actinide and lanthanide solid phases.

As an example, the SEM picture seen in Figure 3(a) shows particles of $\text{NaNpO}_2\text{CO}_3 \cdot 3.5\text{H}_2\text{O}$ that precipitated from a Np(V) solution oversaturated with carbonate. The image clearly shows the crystalline nature of the solid and the lack of amorphous material. An energy-dispersed spectrometer was used to evaluate the chemical composition of those solids, which showed that only sodium, neptunium, and carbon are present in the solid. XPS is sensitive to an element's electronic state and can be used to examine the oxidation state of a metal ion. The oxidation state is revealed by a shift in the binding energy in the XPS photoemission spectra. Figure 3(b) shows that when Pu(IV) compounds sorb onto SiO_2 (one of the simplest metal oxide surfaces), the characteristic $4f_{7/2}$ photoemission peak shifts by several electron volts away from the peak position of metallic plutonium.

(a) SEM



(b) XPS

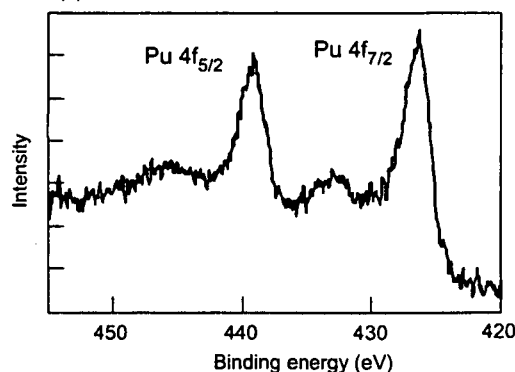


Figure 3. Surface Analysis of Np and Pu Compounds

Figure 3(b) is courtesy of R. Schulze and M. Neu.

X-Ray Absorption Fine Structure (XAFS) Spectroscopy.

The use of XAFS to gather information about the actinides has increased dramatically in the last five years. XAFS is element specific and allows us to deduce speciation without perturbing the sample's original distribution. The spectroscopy can yield information on the actinide's oxidation state, coordination number, bond length, and nearest-neighbor atoms. We have used XAFS to determine those features for solid (amorphous and crystalline) and solvated actinide compounds. Samples typically must have actinide concentrations in the lower millimolar range. More information about XAFS spectroscopy is found in the Conradson's article on page 422.

As discussed above, we used XAFS to identify the predominant plutonium species in contaminated soil at Rocky Flats. This was the first definitive spectroscopic data on plutonium in an environmental sample. The x-ray absorption near-edge structure data (XANES) of the L_2 absorption edge, seen in the graph in Figure 4(a), indicate that the plutonium in the most concentrated samples is in the highly stable and immobile form of plutonium dioxide, PuO_2 . The extended x-ray absorption fine structure (EXAFS)—Figure 4(b)—shows eight oxygen neighbors at a Pu-O distance of 2.33 \AA , consistent with the fluorite structure PuO_2 . The data also show that plutonium is most concentrated in soil layers that are about $0.25\text{--}0.5$ millimeters below the surface, is dispersed on both macro- and microscopic scales, and is not highly associated with any other particular element. These results help Rocky Flats personnel who must address potential plutonium migration paths from the site and remediate the area.

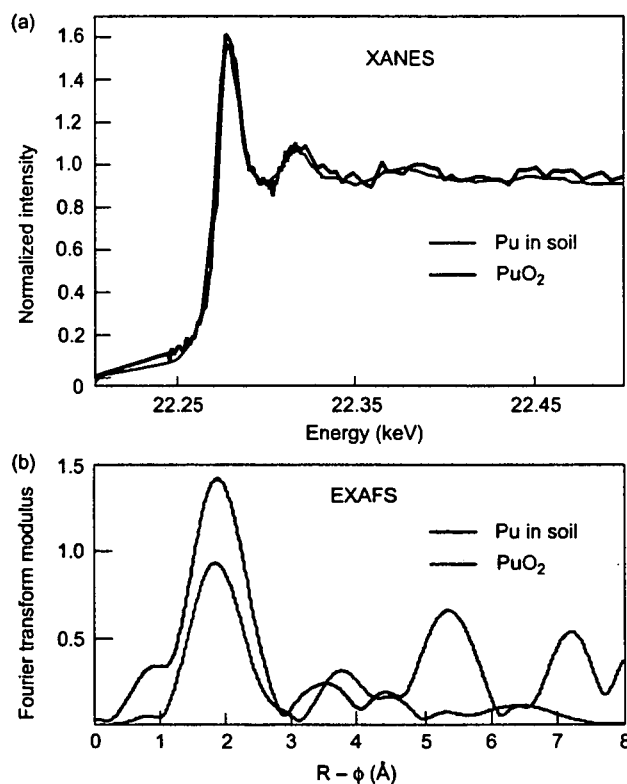


Figure 4. XAFS of Plutonium-Contaminated Soil Sample

22

Nuclear Magnetic Resonance (NMR) Spectroscopy. NMR is a standard analytical method in organic and inorganic chemistry. It is used for probing the electric quadrupole moments or magnetic dipole of some elements, which provides information about the structure and conformation of chemical species. Modern high-field superconducting magnets allow us to investigate the speciation down to millimolar concentrations.

At Los Alamos, we have used ^{13}C and ^{17}O NMR to study the stability of the highly soluble triscarbonato complex, $\text{UO}_2(\text{CO}_3)_3^{4-}$, in NaCl solutions. This U(VI) anion is stable at relatively high carbonate concentrations, but with decreasing pH, the complex protonates and forms the trimer, $(\text{UO}_2)_3(\text{CO}_3)_6^{6-}$. The trimer's structure was determined previously by single-crystal x-ray diffraction and by XAFS spectroscopy. As illustrated in Figure 5, we have used the chemical shifts to characterize and quantify the U(VI) species involved in the chemical equilibrium. The $\text{UO}_2(\text{CO}_3)_3^{4-}$ complex has three equivalent terminal carbonate ligands (see Figure 4(c) in the main text) and thus it produces a single ^{13}C NMR frequency shift at $\delta = 165.6$ parts per million (ppm). The trimer has two different carbonate ligand environments—the outside of the complex (terminal) and between the uranyl ions (bridging)—that give rise to two signals: $\delta = 165.2$ ppm for the three terminal ligands and at $\delta = 166.5$ ppm for the three bridging ligands. By integrating the signal, we obtain the stability constants. These indicate that increasing the ionic strength favors and stabilizes the more soluble triscarbonato complex. Our studies are relevant for the transport behavior of An(VI) in geologic salt formations, such as those at the WIPP site.

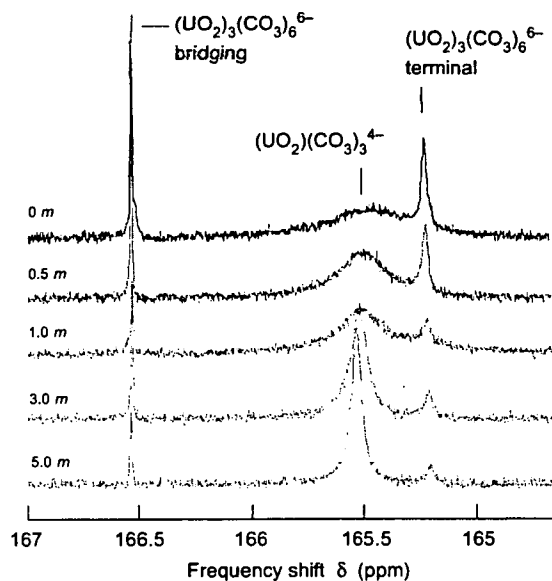


Figure 5. NMR Spectra of U(VI) Complexes

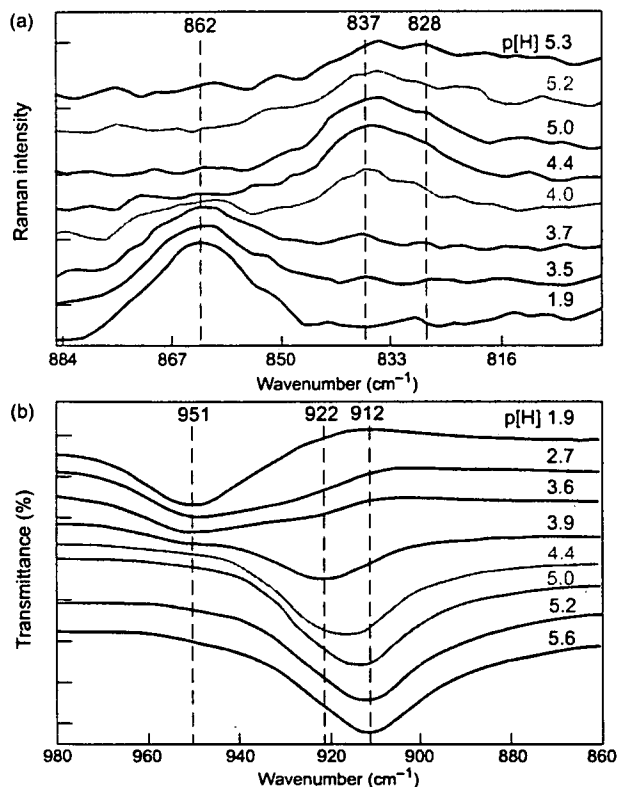


Figure 6. NMR Spectra of U(VI) Complexes

Fourier Transform Infrared (FTIR) and Raman Spectroscopies. These two techniques measure the vibrational spectrum of molecules and provide information on the molecular structure and the characterization of functional groups. We have used them to study the relationship between bond strength and length in An(V,VI) compounds, including U(VI) complexes with hydroxide, chloride, phosphate, or chloride ligands.

As seen in Figure 6(a), the Raman-active symmetric (ν_1) stretch of the UO_2^{2+} ion in solution, normally at 873 cm^{-1} , is shifted to 862 cm^{-1} as coordinated water molecules are replaced with chloride ions in 5-M NaCl. With increasing pH, hydrolysis species can be observed at different frequencies. Interestingly, solution speciation in chloride brines depart significantly from predictions based on previous investigations of U(VI) in non-complexing sodium perchlorate (NaClO_4) solutions. For example, the vibrational frequency of the first polynuclear hydrolysis product $(\text{UO}_2)_2(\text{OH})_2^+$, normally seen at 852 cm^{-1} in NaClO_4 , is not observed in chloride brines because of its lower stability. Instead, the signal for $(\text{UO}_2)_3\text{O}(\text{OH})_3^+$ is observed at 837 cm^{-1} while the tetramer $(\text{UO}_2)_4(\text{OH})_7^+$ appears at 828 cm^{-1} . Analogous shifts of the vibrational frequencies for the $(\text{UO}_2)_2(\text{OH})_2^+$ can be observed in the corresponding FTIR spectra seen in Figure 6(b). The IR frequency of the ion in 5-M NaCl shifts in NaClO_4 solution from 951 cm^{-1} to 961 cm^{-1} , the trimer shifts from 922 cm^{-1} to 924 cm^{-1} and the tetramer shifts to 912 cm^{-1} .

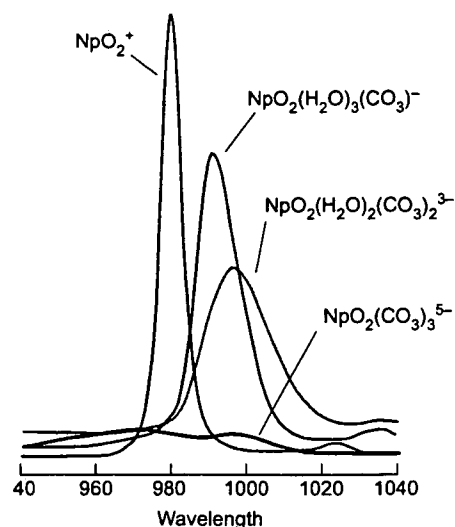
Ultraviolet, Visible, and Near-Infrared (UV-vis-NIR) Spectroscopy.

Absorption studies employing UV-vis-NIR spectroscopy have been widely used to study the complexation reactions of actinides in solution. The technique has a sensitivity down to micromolar concentrations, and actinide species in all oxidation states can be characterized because the actinides exhibit characteristic Laporte forbidden f-f transitions. (See Table I.) Complexation reactions of the non-complexed ion can be tracked because the absorption band is shifted significantly with the addition of ligands. For example, the non-complexed Np(V) aquo ion, $\text{NpO}_2(\text{H}_2\text{O})_5^+$, exhibits a strong absorbance at 980 nm.

As seen in Figure 7, the monocarbonato species $\text{NpO}_2(\text{H}_2\text{O})_3(\text{CO}_3)^-$ absorbs at 991 nm, the bicarbonato complex absorbs at 997 nm, and the triscarbonato complex absorbs at 974 nm. Combining these spectroscopic results with those from XAFS experiments has given us insight into the molecular structures of environmentally relevant Np(V) complexes.

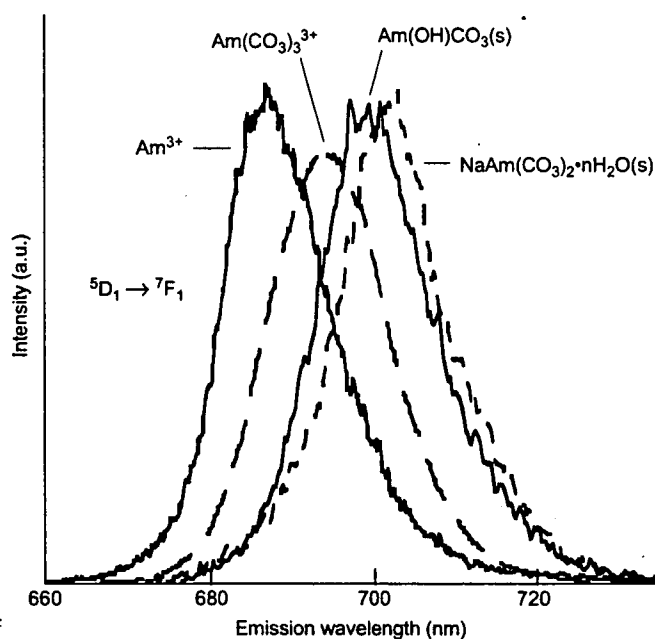
Table I. Characteristic Absorption Wavelengths

Species	Wavelength (nm)
U(IV)	650
U(VI)	414
Np(IV)	960
Np(V)	980
Pu(IV)	470
Pu(V)	569
Pu(VI)	830
Am(III)	503
Cm(III)	400

**Figure 7. UV-vis-NIR Spectra****Laser-Induced Fluorescence (LIF) Spectroscopy (LIF).**

Fluorescence spectroscopy can be used to probe the excited and ground states of only a few actinides species—for example U(VI), Am(III), and Cm(III). The fluorescence decay rate of the emission spectra depends on the nature of ligands that are present in an actinide's inner coordination sphere. When combined with information about the lifetime of non-radiative relaxation processes, LIFS is sufficiently sensitive to probe chemical speciation at nanomolar concentrations.

We have used this method to characterize the environmentally relevant solid and solution compounds of U(VI) and Am(III). As inner-sphere water molecules are replaced with carbonate ligands, the emission wavelength changes. One of the strongest absorption transitions for Am(III) compounds is the $^5\text{D}_1 \rightarrow ^7\text{F}_1$ band at 685 nm, and as seen in Figure 8, the peak emission for $\text{Am}^{3+}(\text{aq})$ (at 685 nm) shifts towards higher wavelengths with carbonate complexation. The fluorescent lifetime of the ion's excited state also increases, for example, from 20.4 nanoseconds for $\text{Am}^{3+}(\text{aq})$ to 34.5 nanoseconds for $\text{Am}(\text{CO}_3)_3^{3-}$. The increase follows the known trend for Eu(III) and Cm(III) complexes. From the measured lifetime of the excited state we determine that there are 11.1 ± 0.5 water molecules around the Am^{3+} ion and 6.0 ± 0.5 water molecules for $\text{Am}(\text{CO}_3)_3^{3-}$. Since the three carbonate ligands bond in a bidentate fashion, our results agree with a coordination number of 12 for the latter complex. Thus far, we have been unable to obtain fluorescence data on the mono- and bicarbonatocomplex due to the low solubility of Am(III) at lower carbonate concentration.

**Figure 8. LIF Spectra**

24/24